Democratic and Popular Republic of Algeria

Ministry of higher Education and Research

University Mohamed Boudiaf of M'Sila

Faculty of Sciences

Department of chemistry

Master Memory

Specialty: Chemical of Materials

Students:

BARKAT Lahcen and BENHAFFAF Abderrahmane

THEME

Synthesis, characterization and electrochemical investigation of CuO films deposited by ultrasonic spray method

2021-2022

Members of the Jury:

President: Pr. Abdelbaki Reffas	University of M'sila
Supervisor: Pr. Yazid Bouznit	University of M'sila
Examiner: Dr. Mahmoud Lebid	University of M'sila

Acknowledgements

First of all, we would like to express our deepest sense of gratitude to our memory advisor, Pr. Yazid Bouznit, for his strong scientific supervision and guidance on our work during all these three months, for his precise and valuable comments on the manuscript.

We would like to express our sincere regards to the jury members, Pr. Abdelbaki Reffas and Dr. Mahmoud Lebid for devoting their precious time to the review of our manuscript and for their scientific evaluation.

DEDICATION

My mother, *who worked for my success, with her love, her support, and her precious advices.*

My father, *who could be proud and find the result of long years of sacrifices to help me move forward in life*

Abdelkamel, *who has never ceased to be for me an example of brotherhood, for everything he has done for my good and happiness.*

To my brothers, Sohieb, Dido and my little sister Fatma Zohra

To all those who have helped me from near or far, they will find in these lines the expressions of my gratitude.

Lahcen

DEDICATION

To my dear mother who has never stopped sparing her efforts for me to reach this level. His sacrifices and deprivations did not prevent him from fulfilling his duty to mother concerned about her children's future

To my dear father who was patient, understanding and encouraging, her fatherly warmth has been and will always be

for me of great comfort.

To my Brother Mohammed Oussama, who has always been at my sides, supports and encourages me constantly: words will never allow me to thank.

Greetings to all my friends: Islam, Sayf, Lahcen, Hamza, Hicham, Marwan, Aymen

And for a long list

Abderrahmane

Table of content

Table of contents

Table of contents

General introduction

General introduction

In recent years, the industrial revolution and the development of the humanity demand the discovery of new materials and innovative technology in order to make the industrial devices work with less cost, higher efficiency and less pollution.

Today, researchers have drawn attention to the semi-conducting metal oxide nanostructures because of their large field of technological application. Among these metal oxides, copper oxide CuO thin films have attracted a considerable attention for several reasons. In fact, copper oxide tenorite phase CuO has a monoclinic structure which belongs to a crystallographic space group C2/c. It has p-type conductivity because of the existence of copper vacancies in its structure. This oxide has a direct band gap (Eg) and its value depends on the method growth and Eg varies between 1.2 and 2.1 eV which is close to the optimal band gap used for absorber layer in solar cell [1,2]. copper oxide thin films are very useful for different applications in different fields of technology such as gas sensing [3], photovoltaic technology [4], lithium-ion batteries [5] and photo catalysis. [6]

In order to synthesize copper oxide thin films, a variety of deposition techniques can be used such as sputtering [2], spray pyrolysis [1], thermal oxidation [7], chemical vapor deposition (CVD) [8] and sol-gel [6]. In this present study, CuO thin films were deposited on glass substrates using the spray pyrolysis technique which is a simple and a low-cost technique with high deposition surface, in order to investigate the influence of thickness and annealing in air on structural, optical and electrical properties of the resulting films.

The prepared films were characterized by different characterization technique such as: X-ray diffraction (XRD), scanning electron microscope (SEM), Electrochemical Impedance Spectroscopy (EIS), chrono-ammeter and Mott-Schottky.

Chapter 1

Chapter 1 « Generalities »

1. Metal oxides

1.1. Definition

Metal oxides are crystalline solids that contain a metal cation and an oxide anion. They typically react with water to form bases or with acids to form salts.

The alkali metals and alkaline earth metals form three different types of binary oxygen compounds: (1) oxides, containing oxide ions, O^{2-}, (2) peroxides, containing peroxide ions, O_2^{2-}, which contain oxygen-oxygen covalent single bonds, and (3) superoxides, containing superoxide ions, O^{2-}, which also have oxygen-oxy

gen covalent bonds but with one fewer negative charge than peroxide ions. Alkali metals (which have a +1 oxidation state) form oxides, M_2O, peroxides,M_2O_2, and superoxides, MO_2. (M represents a metal atom.) The alkaline earth metals (with a +2 oxidation state) form only oxides, MO, and peroxides, , MO_2. All the alkali metal oxides can be prepared by heating the corresponding metal nitrate with the elemental metal**.[09]**

A metal oxide is a body made up of metallic atoms and atoms Oxygen ($M1_x\ M2_y\ O_z$) where M is the chemical symbol of the metal atom under consideration, O the symbol of the oxygen atom, “x” and “y” and “z” of the natural integers.

Examples:

Oxides of copper: CuO, copper oxide II

Tin oxide : SnO_2 tin dioxide

Zinc oxide : ZnO.

We can classify metal oxides, either according to the nature of the conduction by electrons or holes, or depending on whether the metal oxides are simple or complex.

1.2. Types of metal oxide

There are two large families of metal oxides (Table 1). The first types p (hole conduction). They are known to be relatively unstable due to their tendency to exchange oxygen from their network easily with air. However, the types «p» are used for certain applications such as high oxygen sensors temperature **[10] [11]**

The second family consists of the “n” types (electron conduction). They fill the majority of gas sensor applications, as they are more stable and have properties more favorable to chemisorptions.

Métal oxyde type n	**Métal oxyde type p**
SnO_2	NiO
ZnO	CuO
TiO_2	La_2O_3
In_2O_3	$BaTiO_3$
Ta_2O_5	Ag_2O

Table 1. *List of major metal oxides.*

1.3. Simple and Complex Metal Oxides

Metal oxides are classified into two main categories: metal oxides which are made up of a metallic atom such as: SnO_2, TiO_2, SiO ,,,,,,, and oxides mixed metal consisting of two or more metallic atoms such as: $BaTiO_2$, $CaTiO_3$, $Mg_2\ SiO_4$

1.4. Application of Metal Oxides

Metal oxides play a key role in environmental remediation and pollutant sensing and are strategic also in several other applications including energy production, conversion and storage. Metal oxides exhibit a great variety of functional properties, strongly depend ending on their crystal structure, morphology, composition, intrinsic defects, doping, etc., which determine their optical, electrical, chemical and catalytic properties. Growth methods and process parameters strongly govern the morpho-structural characteristics and therefore the physico-chemical properties of metal oxides **[12, 13].** The band gap and electronic structure of oxides can be controlled and tailored by the size and dimension and this is the key to multifunctional possibilities presented by metal oxide-based materials. Modulating the band gap and surface adsorption properties is essential for application in heterogeneous photo catalysts. The structural diversity of metal oxides is provided by both chemical and physical methods of synthesis, and by the process parameters. A lot of work has been reported in the green synthesis of metal oxide-based materials **[14].** Recently, metal oxides' synthesis assisted by ionic liquids (ILs) has been proposed to achieve oxides' production with controllable nanostructures (nanorods, nanospheres, core-shell nanostructures, etc.) and increased catalytic efficiency for air pollutant sensing and remediation. ILs ability to dissolve inorganic compounds can play a noteworthy role in producing highly dispersed composites, enhancing their activity **[15].**

The release of toxic and often difficult to degrade chemicals from industries producing pharmaceuticals, textiles and paints leads to large-scale water and soil pollution. In this regard, metal and metal oxide nanoparticles have been known to exhibit good photo catalytic properties for the degradation of such chemicals. An environmental remediation photo catalyst works by facilitating oxidation and reduction processes via trapping the light energy which leads to quick degradation of the targeted pollutants. Apart from common

organic pollutants like dyes, other organic pollutants like antibiotics, PAHs, pesticides, and non-organic species such as heavy metals, radioactive metal compounds, sulfur compounds, and inorganic contaminants also need to be removed from water bodies. Environmental remediation also involves effective measures to monitor the levels of these pollutants in soil, water and air **[16].**

Concerning the energy applications, the photo electrochemical (PEC) water splitting and the photo catalytic reduction of CO_2 represent environmentally friendly and sustainable sources of hydrogen fuel and renewable fuels and chemicals, respectively. Metal oxide semiconductors play a key role in both applications, due to their photo-electrochemical stability, low cost, favorable band edge positions and band gaps.

The present review deals with the recent advances in photo catalytic applications of selected metal oxides for pollution remediation and energy production. The study highlights how metal oxide are used in applications for energy and environmental sustainability, taking into account also the limit of their practical application on large scale.

- *Métal Oxyde-Based Materials*
- Global indicators of sustainable development (evaluation of the influence of the human development index on consumption and quality of energy) were recently contributed by one of the authors of this manuscript **[17, 18].**
- The applications of some of the representative metal oxide-based materials, characterized by different nanostructures, are shown in **Table 2**. The list of oxides reported in the table is not exhaustive, and the photo catalytic performances of many other metal oxides will be be discussed in the next sections. As evident from the data presented in **Table 2**, the structure of the core and the functional materials are important in modulating the band gap and the surface adsorption properties of these heterogeneous photo catalysts.

- Band gap modulation, microstructure and optoelectronic properties are fundamental for a wide range of metal oxide applications **[19].** The structural diversity of metal oxides is provided by the method of synthesis among which the most common are co-precipitation, deposition, hydrothermal method, sol-gel method, soak–deoxidize–air oxidation, and impregnation.

Métal Oxyde-Based Material	**Structural Features**	**Synthèses Méthode**	**Application**
ZnO nanosheets	3D hierarchical flower-like architectures	Solvothermal	Adsorption of triphenylmethanedyes
Fe_3O_4UiO-66 composite	CubicalNPsarranged	Sonication	Adsorption
Fe_3O_4MIL-100(Fe) Core–Shell Bionanocomposites	Core-shell structure with Fe_3O_4 core, immobilized on P. Putida	Sonication followed by attaching the NPs on bacteria	Adsorption
ZnO–TiO_2/Clay	TiO_2 and ZnO NPs mounted on clay surface	Sol-gel méthode	Degradation of MG
Cu/ZnO/Al_2O_3	Cu and ZnO impregnated γ-Al_2O_3	Impregnationmethod	CO removal from reformed fuel
Co^{2+}, N^{I2+} doped Fe_3O_4 NPs	Cubic lattice	Co-precipitationmethod	Photo degradation of Carbol Fuchsin
Ce/Fe bimetallic oxides (CFBO)	Flowerlike 3D hierarchical architecture	No-template hydrothermal method	As(V) and Cr(VI) remediation
Perovskite titanates ($ATiO_3$, A = Sr, Ca and Pb)	Leaf-architectured 3D Hierarchical structure	Combination of biosynthesis from Cherry Blossom, heating, grinding and photodeposition	Artificial Photosynthetic System for photoreduction of CO_2
TiO_2 polypyrrole	Coreshellnanowires (NWs)	Seed-assisted hydrothermal method	Flexible supercapacitors (SCs) on carboncloth
Fe_3O_4/WO_3	HierarchicalCoreshell Structure	Solvotermalgrowth + oxidation route	photodegradation of organic-dye materials

Table 2. *Applications of some representative metal oxide-based materials with various structures.*

Possible applications of metal oxides

_ Environmental remediation

_ solar cells

_ photovoltaic applications

_Nanoelectronic devices

_clean energy production

_biological uses

_sensors

Fig. 1 Possible applications of metal oxides.

1.5. Copper oxides Cu_2O and CuO

The two main copper oxides correspond to the oxidation state (**Cuprite** $\boldsymbol{Cu_2^{I}O}$) and the oxidation state II (**Tenorite** $\boldsymbol{Cu^{II}_2O}$) of copper.Note that it exists also a third copper oxide called paramelaconite ($\mathbf{Cu_4O_3}$). This oxide corresponds to a mixed valence of copper $\mathbf{Cu^{I}Cu^{II}}$ It is metastable and therefore very little **[20]**

1.6. Applications of CuO

CuO first attracted attention of chemists as a good catalyst in organic reactions but recently discovered applications of CuO such as high-Tc superconductors, gas sensors, solar

cells, emitters, electronic cathode materials also make this material a hot topic for physicists and materials science engineers. Some of the most interesting applications of CuO nanomaterials are sensing, photo catalyst, and super capacitor that will be highlighted in this section.

1.6.1. Sensing Applications

It is surface conductivity that makes CuO an ideal material for semiconductor resistive gas sensor applications and in fact CuO nanomaterials were used for detection of many different compounds such as CO, hydrogen cyanide, and glucose. As sensing properties closely relate to the chemical reaction on the surface of sensor, the specific area is a key factor to achieve high sensitivity sensor. Due to the high surface area/volume ratio, the sensing property of CuO nanomaterials was enhanced greatly. The shape of CuO nanostructures was also believed to affect significantly the sensing properties of CuO nanomaterial; for example, spherical crystals often show higher sensitivity than columnar one.

Aslani and Oroojpour **[21]** studied CO-sensing properties of different CuO nanoparticles prepared by solvothermal route as a function of morphology and size of nanoparticles. The results show that cloud like structures with high surface area/volume have higher response and detection limit than other morphologies. Yang et al. **[22]** also showed that the specific surface area of these CuO nanostructures plays an important role in the sensitivity for detecting HCN. Both sides (5 mm in diameter) of a silver-coated quartz crystal microbalance (QCM) resonator were covered with CuO nanostructures; the resonator was used as sensing probe in a quartz crystal resonator. The absorbance of HCN gas on sensor is indicated by the shift of resonant frequency. As specific area of CuO nanostructure used for coating the probe changes from 9.3 m2 /g to 1.5 m2 /g, the sensitivity reduces from 2.26 to 0.31 Hz/μg. In both reports, the authors showed that the sensitivity of sensors depends not only on the

surface area but also on the morphology of the nanostructure. The change in sensitivity of different nanostructures could be explained by the variation in the chemical reactivity of different crystal planes.

Glucose detection is another important application of CuO in sensing field. In conventional methods, glucose detection is based on the use of glucose oxidase which is an enzyme used in the sensor. This enzyme catalyzes the oxidation of glucose to gluconolactone and simultaneously produces H_2O_2. Glucose level is then evaluated by estimation from electrochemical response to the liberated H_2O_2. However, the main disadvantages of conventional methods are high cost and lack of enzyme stability, complicated immobilization procedures of enzyme, and the coexisting interferences in the biological fluids together with critical operating conditions. Most of those limitations could be solved by using CuO nanostructures as an alternative oxidase, where CuO nanomaterials act as catalyst to convert glucose into gluconolactone and finally to glucose acid. The better efficiency of the oxidized reaction in CuO based sensor resulted from high surface area, surface energy which enhanced electron transfer ability of CuO nanomaterials.

1.6.2. Supercapacitors and Electrodes for Lithium Ion Batteries

Pseudo capacitors also known as one type of super capacitors have attracted significant attention of researcher as efficient energy storage devices with superior properties such as high power density, excellent reversibility, and long cycle life time dependent power, which are necessary properties of electronics portable devices. As the demand for high capacity energy storage in modern life was raised continuously, pseudo capacitors have become a hot topic recently. Among transition metal oxides which are considered as ideal electrode materials for pseudo capacitors, CuO is a really promising candidate for its abundant resources, environmental compatibility, cost effectiveness, and favorable pseudo capacitive characteristics. It was found that the morphology and particle

size of CuO remarkably affected its specific capacity. Cauliflower like, nanobelt-shaped, and feather-like CuO nanocrystals were synthesized by the chemical deposition method by group of H. Zhang and M. Zhang **[23]**. According to the authors, morphologies of the CuO nanostructures can influence the electrochemical properties significantly. The electrochemical properties of CuO as electrode material were enhanced by the improving of morphology. Cauliflower-like CuO exhibited a higher specific capacitance than nanobelt-shaped and feather-like CuO and also showed good reversibility. Specific capacitance of cauliflower-like CuO was 343.5% higher than CuO bought at 5 mA cm−2. The CuO cauliflower-like exhibited a higher utilization efficiency and better property for electrolyte diffusion than the feather-like and nanobelts structures. The increasing order of the specific capacitance was consistent with increasing sequence of CuO specific surface area, indicating that the highly mesoporous structure and high specific surface area of the electrode facilitate the ions to transfer into the porous structure more easily which would lead to more redox faradic reactions and surface adsorption of electrolyte cations. CuO nanomaterials could substitute for graphite anode in LIBs due to its superiorities such as high theoretical capacity (670 mAhg−1), improved safety, low cost and environmental benignity. However, it also suffers very rapid capacity decay caused by huge and uneven volume variations (around 174%) during the lithium uptake/releasing process. One possible approach to improve the electrochemical performance of CuO materials is to use well-configured nanostructures ranging from zero-dimensional nanoparticles to multidimensional assemblies. In these nanostructures, not only lithium diffuses much easier, but also the strain associated with lithium uptake could be well accommodated, leading to better electrochemical performance. Wang et al. **[24]** successfully prepared nanorods and nanosheets on a Cu substrate. The unique nanostructural features endower them excellent electrochemical performance with high capacities of 450– 650 mAh g−1 at 0.5–2 C and almost 100% capacity

retention over 100 cycles after the second cycle. Recently composite material of CuO nanomaterial was developed to further increase the capacities of LIBs. Rai et al. **[25]** successfully used CuO/reduced graphene oxide nanocomposite as anode materials for lithium ion batteries. The initial discharge capacity of the pure CuO nanoparticles and their nanocomposite is 785.2 mAh g−1 and 1043.3 mAh g−1 with reversible capacity retention of 392.1 mAh g−1 and 516.4 mAh g−1 after 45 cycles, respectively.

1.6.3. Photo catalyst and Solar Energy Conversion

Water pollution due to organic wastage from industry production has become a serious problem in the world today. Most of organic compounds in waste water are toxic and cannot be decomposed naturally so they need to be treated with care before disposal.

Water treatment using semiconductor catalysts under solar UV or visible light seems to be the most effective way as it has shown that this method could be employed to totally decompose many different organic compounds into biodegradable without complex technologies. CuO is a promising candidate due to low cost and abundance. As a p type semiconductor of narrow band gap in visible region, CuO is expected to be a good material for application in photo catalyst and solar energy conversion. However, some groups reported that CuO shows almost no or very little photo catalyst properties under visible light. Adding some amount of H_2O_2 could help to greatly improve the photo catalyst efficiency under visible light. Yecheskel et al. study the degradation of brominated flame retardants by copper oxide nanoparticles and saw that adding an amount of H_2O_2 enhances the photo catalyst properties of CuO nanoparticles **[26].** They also showed that the interaction of CuO nanoparticles with H_2O_2 results in an electron spin resonance spectrum similar to spectrum of Cu^{2+}+ ion. This fact might indicate a release of Cu^{2+} ion to the solution or changes in the electron configuration of CuO nanoparticles in the solid phase. Based on these effects, the authors suggested that H_2O_2 may have a role in the activation of

CuO catalyst besides being an oxidative agent. It is noteworthy that photo catalyst properties also show dependence on size and shape of CuO nanostructures which again can be explained by the enhancement due to large surface area as well as the anisotropic of single crystals nanostructures of CuO, meaning that the photo catalyst of different crystal plane in CuO could be different. CuO could also be good candidate in solar energy conversion due to many properties: high absorption coefficient, narrow band gap in visible region which is expected to give high conversion efficiency, being nontoxic, stability, good electrical conductance, simple manufacture process, and so on. A more direct way to convert solar energy to electricity is to use CuO as absorber in solar cell. Efficiency of solar cell based on CuO is far lower than efficiency of leading chalcogenide system such as CIS or CIGS, but due to its low cost, abundant resource, and simple preparation process it was shown that efficiency of only several percents in cell based on CuO is good enough to make commercial solar cells. Different from its counterpart Cu2O, CuO is used less for solar cell as the achieved efficiency for Cu2O is higher. Number of reports on CuO solar cell is rare but recent results show very promising achievement, which shows that further development of CuO nanomaterials based solar cell has a bright future. Kidowaki et al. **[27]** prepared solar cells based on CuO nanoparticles/C60 junction which provided efficiency η of 1.8 × 10−6%, fill factor of 0.25, Jsc of 0.18 × 10−3 mA cm−2 and Voc of 0.04 V. A crystallite size of CuO was determined to be 3.4 nm, and higher crystallinity of CuO would increase the efficiency of the CuO/C60 solar cells. Or more recently, using solvothermal method, Chandrasekaran **[28]** prepared CuO nanoparticles and used the product to make a solar cell with efficiency of 0.863%, which is compared with other reported values **[29]**. Up to now, the record efficiency of solar cell based on copper oxide is about 2%, while the theoretical value is about 20%, so efficiency of several percents is obviously achievable. CuO nanomaterials could also be used as good substitution for expensive noble metal cathode in dye solar cell. This topic was first

introduced by Anandan et al**. [30]** in 2005 and the optimal power conversion efficiency when using CuO nanorods as electrode was 0.29% compared with 1.23% when using Pt as electrode in the same condition. By using CuO nanoneedles of higher surface active area, Liu et al**. [31]** obtained an efficiency of 1.12%, for TiO_2 based dye solar cell. This result shows that nanomaterials of CuO could replace well Pt electrodes and can even give better efficiency under optimization process.

1.6.4. Field Emission Effect

Field emission displays are now in a more dominant position in the market compared with CRT displays because of their advanced properties such as high brightness, good color rendition, short response time, and low power consumption. Among the various nanomaterials studied for field emission applications, 1D nanostructures of CuO emerged as very promising field emitters because of some advantages: low turn-on field, high current density, and low fabrication cost **[32].** Liu et al. **[33]** investigated the field emission properties of an individual CuO nanoneedle by in situ microscopy. The authors showed that individual nanoneedle possesses good field emission properties, such as low turn-on field of 5.3 V/μm, high maximum current of 1.08 μA at 9.7 V/μm. The field emission properties of the single CuO nanoneedle and CuO nanoneedle's film arrays are also compared and the results showed that the screening effect played a key role in the field emission properties. Hu et al. **[34]** used a simple method of direct heating of bulk copper plates in air to obtain CuO nanowire films on a large scale. The length and density of nanowires could be controlled by growth temperature and growth time. The as produced CuO nanowires have high density, good preferred orientation, and sharp tip, which is very beneficial to field emission. Field emission measurements showed that CuO nanowires have a low turn-on field of 3.5–4.5 V/μm−1 and a large current density of 0.45 mA cm−2 under an applied field of about 7 Vμm−1. The authors also showed that CuO nanowires having large length/radius

ratio can effectively improve the local field, which enhance field emission. Zhu et al. **[35]** prepared some different CuO nanostructures by solution method. By varying the oxidant concentration, the authors can modulate the morphology of the nanoproducts from nanorod to nanotubes. The tip morphologies of CuO nanostructures were found to be crucial for the field electron emission, and the nanorods with needle-like tips showed superior emission properties with a turn-on field of 3.5 V/μm and a field enhancement factor of 2107, compared to other structures.

Apart from improving the field emission efficiency by optimizing the aspect ratio (length/diameter) of 1D nanostructure, some other methods were also utilized to enhance the field emission current. Wang and Li **[33]** found that laser irradiation could effectively enhance the field emission current of CuO nanowire arrays. The effects of laser intensity, wavelength, and emission current, and working vacuum on the enhancement have been investigated in detail. Among these factors, the contribution from extra excited electrons, which increases the number of electrons in conduction band of CuO for subsequent tunneling, is dominant. The observed laser induced enhancement in field emission current is attributed to the interplay of two factors, namely, laser induced electron transition to excited states and surface oxygen desorption. Based on the idea of light induced field emission of their work, new vacuum nanodevices of CuO nanowires such as photodetectors or switches could be developed in the future. Another example is the work of Maji et al**. [36],** where the authors also prepared CuO nanowire arrays by thermal oxidation. In order to improve the field emission properties of CuO nanowires they coated a ZnO layer on a Cu substrate before the thermal oxidation process. The ZnO layer was deposited by immersing a Cu foil into an aqueous solution of zinc nitrate and hexamethylenetetramine at 95◦ C for several hours. The turn-on field of the ZnO-coated CuO nanowire array was 0.85 V/μm compared with turn-on field 6.5 V/μm of CuO nanowires without ZnO coating layer at the

same current density of 10 μA/cm2. The authors suggested that in addition to the enlarged nanowire density and aspect ratio, crack elimination may be the reason for the 2enhancement of field emission properties.

2. General properties of solid state semiconductors

2.1. Definition

Semiconductors are materials whose conductivity is intermediate between that of drivers (~ 10 Ω^{-1}. cm^{-1}) and insulators (~10^{-22} to~$10^{-14}\Omega^{-1}$. Cm^{-1}) varies with temperature and presence of impurities **[37].**

2 .2 Optical absorption spectra and band gap

The morphology and structure of nanoparticles can modify their electronic and optical properties. The UV-Visible absorption spectra and band gap spectra (Tauc's plot) of Sr-doped CuO nanoparticles the absorption maximum mainly depends on the size of the nanoparticles. In the case of nanoparticles having lower size range, the absorption maximum will get shifted to lower wave number and hence Srdoped CuO nanoparticles have higher band gap compared to bulk CuO. The spectrum shows the band edge-absorption peak which is at 294 nm. The best linear relationship is obtained from Tauc's plot **[33,34]** by plotting (αhv)1/2 against hv indicating the optical band gap of the Sr-doped CuO nanoparticles is due to a direct allowed transition. The band gap is determined from the intercept of the straight line at a = 0, which is found to be 3.1 eV. This bandwidth is very much greater than that of bulk CuO which is 1.85 eV reported by El-Trass et al. Thus, it can be inferred that Sr- doped CuO can be activated by visible light **[38].**

2 .3 Semiconductor type (n) “donor” and (p) "acceptor"

Semiconductor electronic devices have revolutionized countless aspects of human life, from communication and automation to sustainable energy harvest and illumination **[39].** Central to this development is the p-n junction, discovered by Russell Ohl in 1940 **[40].** Through its ability to direct charge flow, the p-n junction can be considered the elemental building block for a range of semiconductor devices, including light emitting diodes, solar cells and transistors. In first generation solar cells, positively and negatively doped bulk high purity silicon typically make up the p-type and n-type sides of the junction, respectively. However, with the increasing utilization of semiconductor devices in modern society, e.g. in the infrared or X-ray energy ranges inaccessible by silicon, the demand for p-n junctions comprised of increasingly exotic semiconductor materials is constantly on the rise. When designing p-n junctions, great care must be taken to control charge densities of the p-type and n-type materials, as well as to match energy levels, in particular band edges. For bulk heterojunctions, where the p-type and n-type materials are based on different semiconductors, chemical compatibility and lattice matching are also very important in order to avoid heterojunction interface recombination and asymmetric expansion during traditional device assembly **[42]**. A homojunction, containing p-type and n-type materials based on the same semiconductor, simplifies many of these requirements, as lattice parameters and band edges already match while the Fermi level, EF, varies slightly due to doping. The selection of contacts is also greatly simplified for a homojunction. In a heterojunction, the difference in band gap between the p-type and n-type materials can be large, which could call for one contact with an extremely high work function and another contact with extremely low work function to inject and extract current. Metal contacts with very low work functions, such as calcium or strontium, are not very stable and are susceptible to oxidation **[38]**. A homojunction bypasses these challenges, and only requires

contacts with work functions varying slightly around the band edges. In bulk semiconductors, controlled addition of aliovalent dopants has become standard procedure to control charge density, for example through phosphorus or boron doping of high purity silicon via energy intensive annealing. Albeit much utilized, this technique results in spatially inhomogeneous doping, and often introduces undesirable scattering mechanisms **[43]**. Another widely adopted technique is ion implantation, which can cause undesirable physical and chemical transformations in the host material owing to impingement of high energy dopant ions. This includes damage to or destruction of the crystal structure and even nuclear transmutations with ions of sufficiently high energy. However, there is limited band gap flexibility when relying on only one bulk semiconductor, unless costly crystal growth methods are utilized to accurately control the chemical composition such as in mercury cadmium telluride, Hg1-xCdxTe **[44]**. Bulk materials are also generally rigid, limiting usage on flexible surfaces. The development of quantum confined nanomaterials opened a new avenue for controlling band gaps in semiconductor materials. Available through solution-based synthesis, colloidal nanocrystals of a range of semiconductors can be fabricated with tremendous size and shape control, using less energy intensive techniques and at a lower cost than analogous methods. The ease of process ability includes ease of upscaling and use of flexible substrates. However, although some band edge tuning has been demonstrated, controllable doping of these nanomaterials has proven to be challenging **[45,46].** In our previous work **[43]**, we demonstrated interfacial sulfur doping of colloidal tellurium (Te) nanowires (NWs) as a remarkably straightforward way to tune p-n type transport in a nanocrystalline semiconductor material. Through high-angle annular dark-field scanning transmission electron microscopy (HAADF-STEM), in combination with X-ray photoelectron spectroscopy (XPS) measurements and energydispersive X-ray (EDX) maps, we showed that sulfur dopant atoms are located primarily on the surface of the NWs. Through DFT

calculations supported by ultraviolet photoelectron spectroscopy (UPS) studies, a mechanism was proposed where the surface sulfur dopants introduce a dopant band just below the conduction band of Te as well as a shift of the EF from close to the valence band edge to the conduction band, resulting in n-type transport. In this work, we revisit this facile surface engineering technique applied to more technologically relevant colloidal bismuth telluride (Bi2Te3) NWs and show that the p-n type transport can be controlled by surface doping with sulfur atoms for low diameter NWs. Bi_2Te_3 NWs were synthesized following a published route **[47],** and surface treatment followed the technique described by us **[43]**. Large and small diameter NWs were synthesized in order to investigate the effect of characteristic size followed by interface engineering. As-synthesized and doped NWs were studied using a battery of techniques: Transmission electron microscopy (TEM), X-ray diffraction (XRD), energy-dispersive X-ray spectroscopy (EDS) and XPS was utilized to investigate changes in NW size, crystallinity, and crystal structure and element distribution. Thermo power (See beck coefficient) and transistor measurements were conducted to evaluate the p-n transition. Our observations confirm the versatility of this surface engineering technique as a facile method to tune p-n type transport in a nanocrystalline colloidal semiconductor material.

3. Thin films

Thin films, material layers with thicknesses between fractions of a monolayer and several micrometers, are ubiquitous today and can be found more or less everywhere. Thin films are applied to modify or enhance the surface of a material or to build functional devices such as light emitting diodes. A small selection of applications where thin films are used are; eyeglasses, microelectronics, drill bits and cutting tools, solar cells, mirrors, flat screens and windows.

The properties of a film and thereby its area of application is, of course, mainly determined by the choice of material. But the structure of the film on a nanometer scale or micrometer scale, known as the microstructure, can also affect the film properties substantially**.** With most thin film systems being polycrystalline1, that is that the film made up by a large number of small crystallites, the microstructure is to a large extent determined by the grain size and morphology and the grain boundary morphology.

3.1. Thin film growth

Thin films go through several distinct stages during growth, each affecting the resulting film microstructure and hence it's physical properties in some, sometimes not reversible, ways. These are the different growth stages of a growing film.

3.1.1 Adatoms and surface diffusion

When an atom or ion impinges on a surface it starts interacting with the surface at a distance of several Å1. It collides with the surface and loses most of its momentum and kinetic energy and lowers its potential energy by adsorbing on the surface. Adsorbed atoms, referred to as adatoms, see a potential energy landscape defined by the atomic structure and chemistry of the surface where adsorption sites of different depth, or stability, are present

3.1.2 The initial stages of film growth

Thin films deposition is performed under far from ideal conditions. Even the best (and very expensive) substrates have rather large densities of surface defects such as vacancies and steps, reactive contaminants are present both in the source material and in the residual gas of the deposition chamber, all while the flux of depositing species is large. Adatoms are therefore bound to encounter sites on the substrate where they are trapped or other

adatoms to which they can bind. All these events result in less mobile or immobile clusters of adatoms, nuclei that form in the first stages of films growth. **[48]**

3.1.2.1 Nucleation:

Adatoms arriving on a perfectly flat surface in the very initial stages of film growth will diffuse randomly until they either encounter another adatom and form a dimer or desorb from the surface. The dimer can, in turn, either grow by the addition of another adatom or dissolve back into two separate adatoms. Larger clusters atoms similarly grow and shrink by attachment and detachment of atoms. However, detachment is unlikely due to the high supersaturation3 encountered in PVD. Clusters consisting of two or more atoms are often stable **[48, 49],** i.e. on average more likely to gain another atom than to lose one from detachment. The critical cluster size, i ∗, is therefore often 1. Different deposition temperatures and other factors such as surface symmetry can lead to critical cluster sizes larger than 1 **[48].**

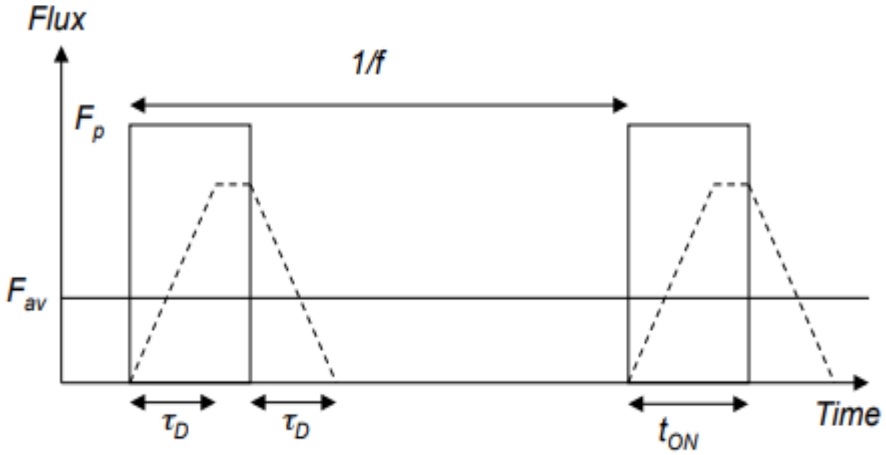

Fig. 2 Idealized picture of pulsed deposition. The solid lines show the deposition flux in the pulse, Fp, and the time-averaged deposition flux, Fav, while the dashed lines show the evolution of the adatom density with τD being the average adatom lifetime.

3.1.2.2. Island growth and coarsening

Several processes take place simultaneously as the nuclei grow and become grains. Atoms continuously attach to, either directly from the vapor or as diffusing adatoms, and detach from the grains with a positive net growth rate for most grains. To understand the processes taking place it is helpful to first consider what happens to a number of differently sized grains on a surface without any deposition taking place. Atoms will constantly detach from an attach to the grains with no net change in size for an isolated grain. Any given grain will therefore be surrounded by a two-dimensional cloud of adatoms at any given moment.

Detachment of an atom from a grain is more probable the smaller the grain is as the binding energy for surface atoms depend on the grain curvature, which is inversely proportional to the grain size. The adatom density around small grains will therefore be higher than around large grains. If two grains of different size are situated near each other there will be a gradient in the adatom density4 between the grains creating a driving force for diffusion from higher adatom density regions around the small grain to the lower adatom density regions around the large grain as shown in figure.3.

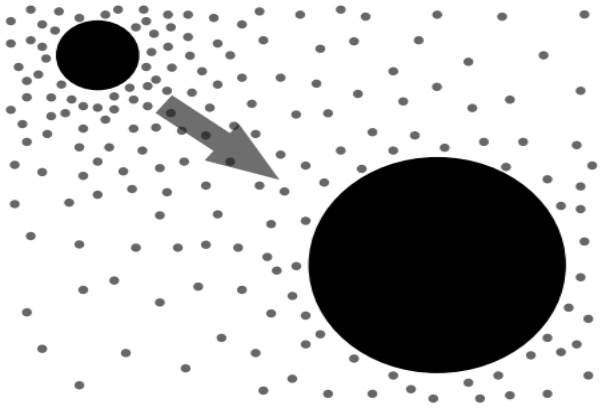

Fig. 3 Schematic of grain coarsening through Ostwald ripening. The large black circles symbolize islands and the small grey circles symbolize adatoms.

3.1.2.3 Coalescence and percolation

The growing islands will eventually meet. As soon as two islands are close enough to interact, they will begin restructuring to minimize the energy in the systems. Impinging islands will deform elastically, touch and form a grain boundary thereby trading surface energy for interface energy and strain energy **[50].** Atoms will diffuse, mainly along the grain surface as bulk diffusion is several orders of magnitude slower, into the neck between the grains to minimize their chemical potential by moving from regions with a positive curvature to the neck which has a negative curvature. Surface diffusion continues to change the grain shape until the new grain reaches its equilibrium shape. Size differences between the coalescing grains will lead to growth of the large grain at the expense of the smaller due to the larger curvature of the smaller grain. One of the consequences of island coalescence is that the areal fraction of the surface covered by deposited material decreases. These newly released surfaces are often large enough to allow for nucleation of a new generation of islands, known as secondary nuclei.

3.1.2.4 Microstructure evolution during film growth

After coalescence the film fully covers the substrate. The structural evolution of the film is now decided by the ability of atoms on the surface and atoms in the grains to move along the grain surface and between the grains. Even though this thesis deals with growth of polycrystalline thin films it's instructive to have a brief look at how single crystalline films grow since the grains in polycrystalline films are single crystals.

- Kinetically limited epitaxial growth: the surface morphology during epitaxial growth is decided by the interplay between material transport between different atomic layers, the interlayer transport, and the nucleation of new islands. **[51]**

- Growth modes from a thermodynamic perspective: The growth mode of heteroepitaxial film is decided by the relationship between the surface energy of the substrate, γs, and the film, γf, and the energy of the interface between the film and the substrate, γi

- Polycrystalline thin films: The microstructural evolution of vapor deposited thin films during growth is highly dependent on the deposition conditions, both those that can be controlled directly and those that cannot. Material deposited at temperatures above or below certain temperature thresholds in comparison to their melting temperature display similar microstructures, see for example **[50,52,53,54].**

3.2. Applications of thin films:

Thin films technology has historically been used in a wide range application going from decorative purposes in its early stage, evolving for optical purposes latter on, and an almost endless range of applications with the appearance of advanced deposition techniques, supported by the rapid development of vacuum technology and electrical power. Overall, thin films are used to enhance the properties of bulk materials by depositing a layer with the desired physical and chemical characteristics to improve their functionality. **[56] [57]**

This table divides thin film properties into five basic categories and gives example of typical applications within each category:

Thin Film Property Category	Typical Applications
Optical	- Reflective/ antireflective coatings - Interference filters - Decoration (color, luster) - Optical memory discs (CDs, DVDs) - Optical Waveguides
Magnetic	- Memory discs (Hard discs and tapes)
Electrical	- Insulation - Conduction - Semiconductor devices - Piezoelectric drivers
Thermal	- Barrier layers - Heat sinks
Chemical	- Barrier to diffusion or alloying - Protection against oxidation or corrosion - Gas/liquid sensors
Mechanical	- Tribological (wear-resistant) coatings Hardness - Adhesion - Micromechanics

Table 3. *Properties and application of thin films*

3.3. Deposition Techniques for thin films:

Thin-films are in general developed to provide special properties, i.e. electrical, optical, mechanical, chemical, that satisfy the needs for specific applications. The desired properties are determined by the resulting film structure, which strongly dependents on the selected deposition method, film material, and substrate. In line with the wide range of applications of thin films, a number of deposition methods have been developed/improved to optimize the film properties, of which, the most commonly employed are described in this section. Broadly speaking, thin-film production can be realized based on two technological groups, namely physical and chemical deposition methods.

3.3.1 Physical deposition methods (PVD)

Physical deposition methods are usually referred as to physical vapor deposition methods (PVD) because the process entails the generation of vapor. PVD essentially consists in removing growth species from a source or target material via evaporation, then this vapor is transported to the substrate surface, and eventually it solidifies in the surface, forming the film. The evaporation is generally carried out under a reduced pressure chamber to avoid impurities in the film formation which are produced due to collisions between vapor particles and residual gas particles in their displacement from the source to the substrate surface. PVD techniques are known to offer a number of advantages, including the deposition of almost any material, high reproducibility of film properties, the use of a large range of substrate materials, the possibility of tailoring the film properties through modification of deposition parameters in single element deposition, and obtaining films with high purity. **[58]** On the other side, among the main disadvantages are the use of sophisticated and costly monitoring systems for the control of the deposition rate and film thickness, and the mismatch between the composition of the deposited film and the composition of the evaporant in the case of alloys and compounds **[59].**

3.3.2 Chemical deposition methods (CVD)

CVD is a deposition method where a volatile compound of a pre-established substance is introduced into a reactor, usually along with an inert gas, to induce a chemical reaction which produces a solid thin film onto a substrate at an elevated temperature. In this technique, unlike PVD, the reaction does not have to be produced under vacuum conditions. Due to its versatility to work with a broad range of reactants and precursors, this technique enables the deposition of a variety of structures, including metal alloys and compound semiconductors with an excellent control of purity and doping (stoichiometric film) **[60]**.

Compared to PVD, this technique offers higher deposition rates, better conformance in rough substrates, easy deposition onto complex surfaces, and high throughput. However, some disadvantages, such as the use of high substrate temperatures, and the toxicity and flammability of the reactive gases have prevented it from being used in lowscaled developments, but is well justified in applications where high-throughput is required, i.e. semiconductor industry. The CVD processes can be classified based on the type of source employed to initiate the chemical reaction, the range of pressure under which the deposition is carried out, and the type of reactant used. **[61]**

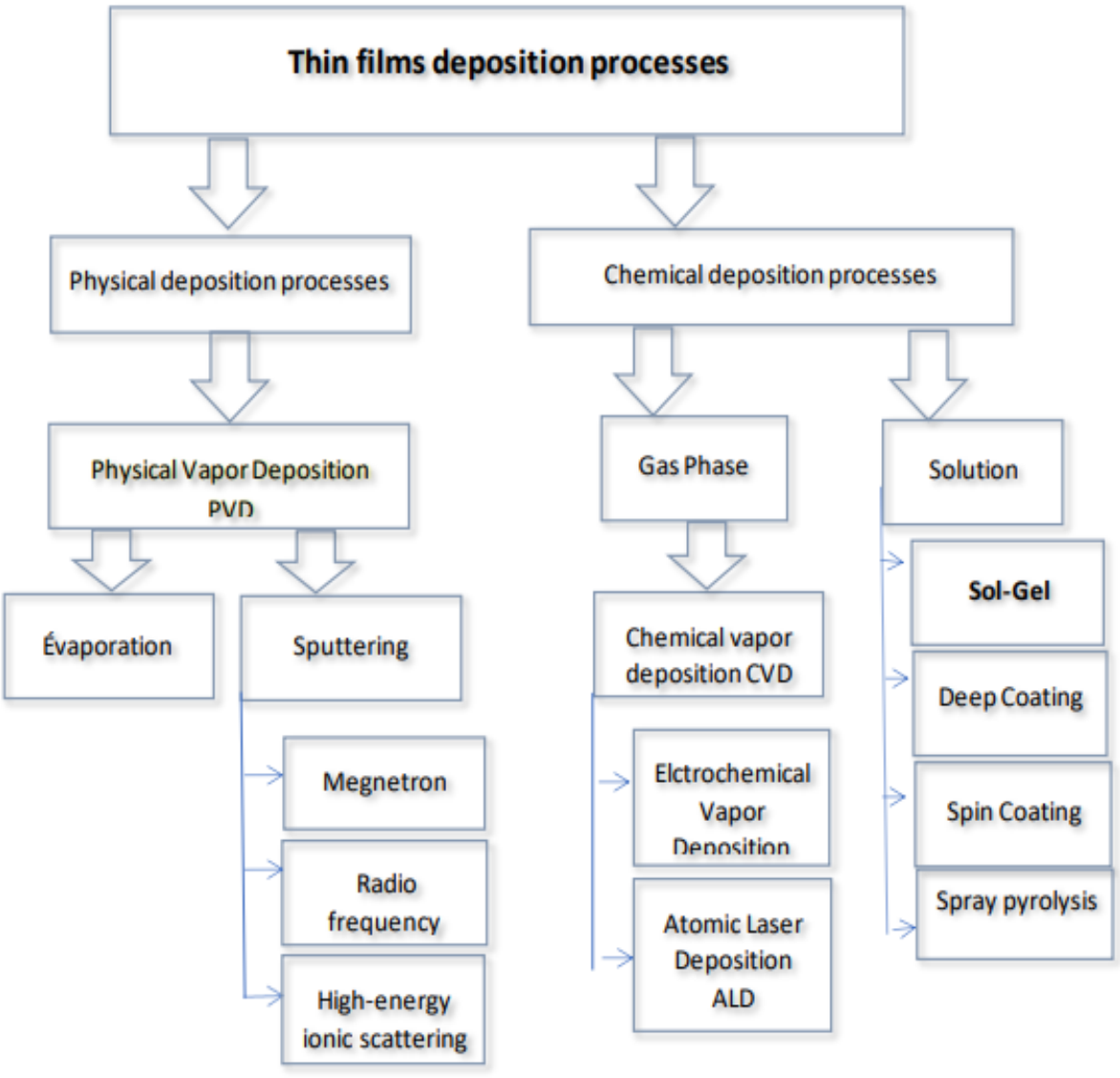

Fig. 4 Thin film deposition

4.Spray pyrolysis technique

Spray pyrolysis has been applied to deposit a wide variety of thin films. These films were used in various devices. It is observed that often the properties of deposited thin films depend on the preparation conditions.

Spray pyrolysis is a processing technique being considered in research to prepare thin and thick films, ceramic coatings, and powders. Unlike many other film deposition techniques, spray pyrolysis represents a very simple and relatively cost-effective processing method. **[62]**

It offers an extremely easy technique for preparing films of any composition. Spray pyrolysis does not require high-quality substrates or chemicals. The method has been employed for the deposition of dense films, porous films, and for powder production. Even multilayered films can be easily prepared using this versatile technique. Spray pyrolysis has been used for several decades in the glass industry and in solar cell production. **[63] [64]**

4.1Working principle:

Chemical spray pyrolysis is a process in which a thin film is deposited by pulverization of a precursor solution in the form of micron dimension droplets onto a preheated substrate where the precursor salts undergo pyrolysis to form a desired chemical compound as an adherent film from more thermally stable compound and volatile by-products evaporates. This process is especially useful for the thin films deposition of metal oxides **[65].**

In the CSP method, thin films are synthesized by nebulizing fine droplets of precursor solutions containing metal salts and different additives (acids, complexing agents etc.) onto preheated substrates. The schematic diagram of the spray pyrolysis system is presented in Figure 3. The typical CSP system is composed of an atomizer, which helps to produce

aerosols, a solution vessel, a heater, and a temperature controller **[66]**.Depending on the atomizer type used, the CSP method can be categorized into three modes: pneumatic, ultrasonic and electrostatic **[65], [67], [68], [69].** Different parameters such as the deposition temperature, carrier gas, solution spray rate, concentration of starting chemicals in a solution, the distance between a spray nozzle and substrates, nature of the substrates and solvents have been reported to influence the film properties **[70].**

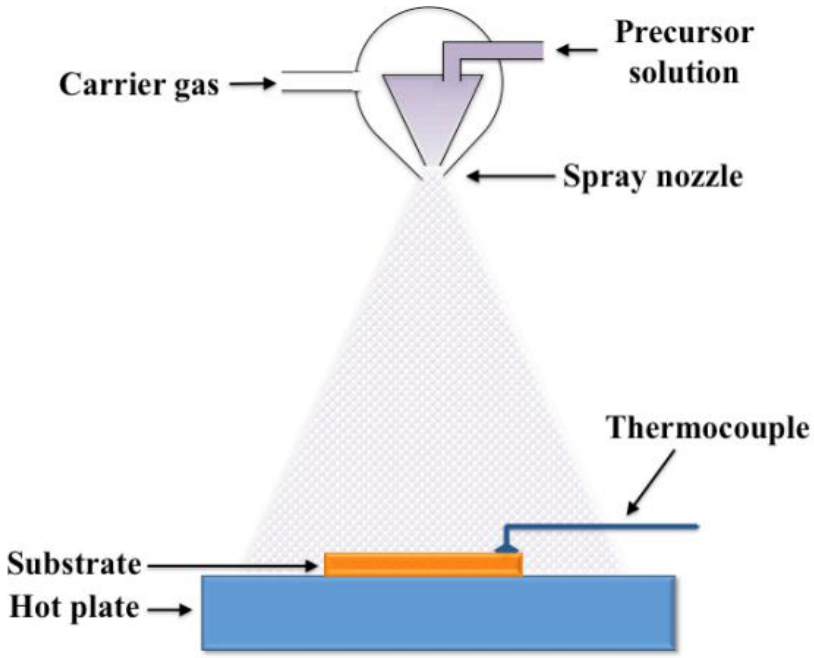

Fig. 5 Schematic of a spray deposition experimental

4.2 Types of Spray pyrolysis technique

4.2.1 PNEUMATIC SPRAY PYROLYSIS

Pneumatic spray pyrolysis belongs to chemical spray pyrolysis which uses pneumatic nebulizer to generate small droplets for the deposition of thin films. It is convenient and simple to use, inexpensive, absence of vacuum, easy to control the composition and

microstructure and can be used for mass production. Despite its advantages, disadvantages include: Difficulties with determination of growth temperature, hard control of aerosol flow rate and film quality may depend on the droplet size and spray nozzle **[65, 66].**

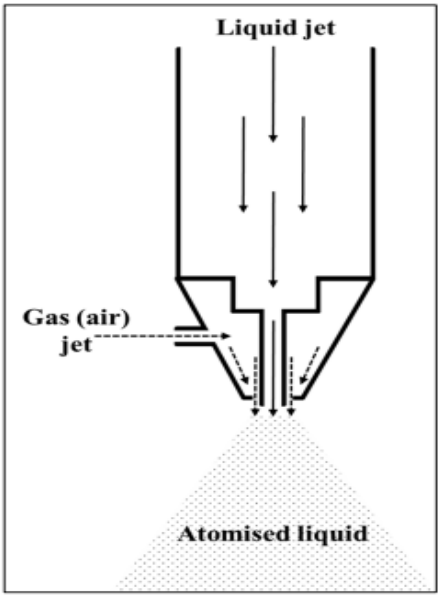

Fig. 6 Diagram showing the breakup of a liquid jet by high pressure gas

4.2.2 ULTRASONIC SPRAY PYROLYSIS

The second type of atomizer is the ultrasonic variety in which a solution is shaken violently as a result of which mists are produced which have a very narrow droplet size distribution **[71].**

In spray ultrasonic, a thin liquid film formed on a high-frequency vibrating surface will break-up in a fine uniform spray. The ultrasonic vibration induces surface waves in the liquid film. As frequency is tuned, very regular square cells can be observed on the free surface just before reaching the resonance frequency (FigI.7). When resonance is reached, the amplitude

grows till droplets break-up (Fig 7). The very regular square cells generate uniform size droplets **[72].**

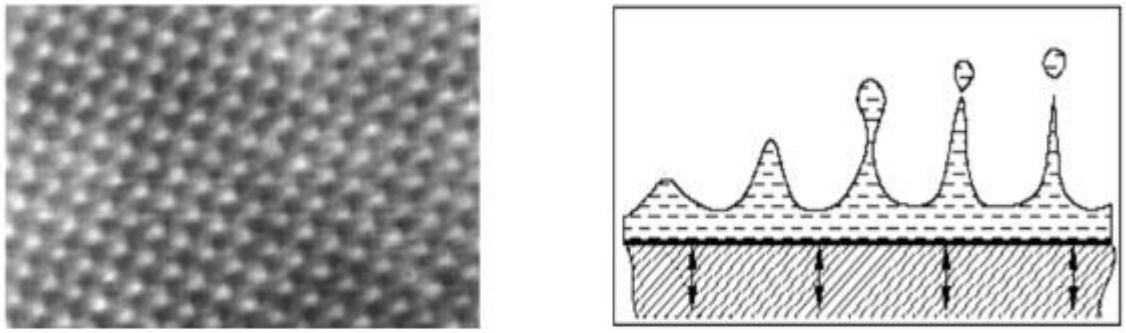

Fig. 7 Standing surface waves patterns during the ultrasonic atomization (water, f=50kHz).

4.3 Advantages of Spray Pyrolysis Technique

The main advantages of spray pyrolysis over other similar techniques are:

- Spray pyrolysis is cost effective and can be easily performed.
- Substrates with complex geometries can be coated.
- Spray pyrolysis deposition leads to relatively uniform and high-quality coatings.
- No high temperatures are required during processing (up to ~ 500 °C).
- Films deposited by spray pyrolysis are reproducible, giving it potential for mass production.

The major interest in spray pyrolysis is due to its low cost, while it is increasingly being used for some commercial processes, such as the deposition of a transparent layer on glass, the deposition of a SnO_2 layer for gas sensor applications **[73]**, the deposition of a YSZ layer

for solar cell applications **[74],** anodes for lithium-ion batteries **[75],** and optoelectronic devices**[76]** .

The composition of the film can be adjusted by changing the precursor solutions. The method used for the deposition of dense films, porous films, and for powder production. Even multi-layered films can be easily prepared using this versatile technique, Spray pyrolysis has been used for several decades in the glass industry **[77]** and in solar cell production to deposit electrically conducting electrodes **[78]**.

One of the major advantages of spray pyrolysis over the vapor-phase routes is the possibility of producing multicomponent particles with exact desirable stoichiometry in the final product.

Chapter 2

Chapter 2« Experimental »

1. Growth process details

1.1. Chemicals used

The Chemicals used for deposition of CuO_2 films are listed in table:

Products	Molar mass (g/mol)	Mass weighed(g)	Involvement
Copper(II) nitrate dihydrate $Cu(NO_3)_2.2H_2O$	**241.55**	**24.16**	**precursor**
zinc acetate $C_4H_6O_4$ Zn	**219.5**	**m (2%)=0,089 m (4%)= 0,182 m (6%)= 0,280 m (8%)= 0,382**	**doping**
Methanol	**32,04**	**-**	**Solvent**
Ethanol	**46,0684**	**–**	**Rinsing**
Hydrochloric acid	**36,46**	**-**	**Rinsing**
Na_2SO_4	**142,04**	**7.102**	

Table 4. *Chemicals used for the preparation of spray solution.*

1.2. Preparation of Solution

To obtain a thin layer of copper oxide, we used tri-hydrated copper (II) nitrate $Cu(NO_3)_2.3H_2O$ as copper source salt and the solvent used is methanol with a molar concentration of 0.2 M.

We prepared a volume of 500ml, then we divided it into five quantities of 100 ml. For each

m (0%) = 0 ; m (2%) = 0.089g; m (4%) = 0.182g; m (6%) = 0.28g ; m (8%) = 0.382g

1.3. Substrates used

Thin film requires a substrate to support itself **[79].** The substrate is very important for the growth of thin films in terms of the lattice and thermal mismatching between it and the film because it commonly leads to the development of stress in the deposited film. The choice of substrate affects crystalline quality as well as optical and electrical properties of ZnO film **[80].**

The thin films of CuO-Cu_2O were deposited on 2 types of substrates which are ordinary glass, glass and FTO. The choice of glass as the deposition substrate was made due to its amorphous nature, surface finish and transparency. We used glass substrates of dimensions 15mm*25mm*1mm. FTO substrates were used to perform electrochemical measurements.

1.3.1 Substrate Cleaning

Substrate cleaning in thin film technology is an important step prior to deposition. It is necessary to remove the contaminants that would otherwise affect the properties of the film. Cleaning involves the removal of contaminants without damage to the substrate. While cleaning, the bond between the substrates is broken and contaminants are set free from the substrates. The properties that can be affected by the presence of contaminants include morphology, nucleation electronic properties and the substrate film interface. Expected contaminants include fingerprints, dust, oil, and lint particles **[81].**

Initially, the substrates were wiped with cotton to remove the visible contamination such as air dust **[82],** then, were successively placed in ethanol and HCl for 05 minutes each. After that they were rinsed with ionized water. Finally, the substrates were dried by compressed air and ready for the spray deposition.

We used the organic solvent ethanol to remove organic impurities, and inorganic solvents (HCl and distilled water) to remove inorganic impurities.

1.4 Experimental conditions

The experimental conditions used during the deposition are listed below:

- Duration of deposit: 50min
- Deposition temperature: 380°C

The deposition procedure comes immediately after the preparation of the substrates and the solutions: the substrate is placed above a heating plate whose power supply is connected to a temperature controller (temperature controller). To avoid thermal shock, the substrates are gradually heated from ambient temperature to the deposition temperature.

When the temperature reaches its set value, ULTRASUNIC is triggered which will cause the precursor solution in fine droplets to the surface of the heated substrate and therefore the oxide layer begins to form.

1.5. Deposition of the spray method

The resulting solution were sprayed in temperature 380°C.Heating the substrate for a minute, then we turn on the ultrasonic device and the spraying process takes place for 50 minutes, with little moving to obtain a homogeneous coating on the surface of the Steel disks (see figure below).

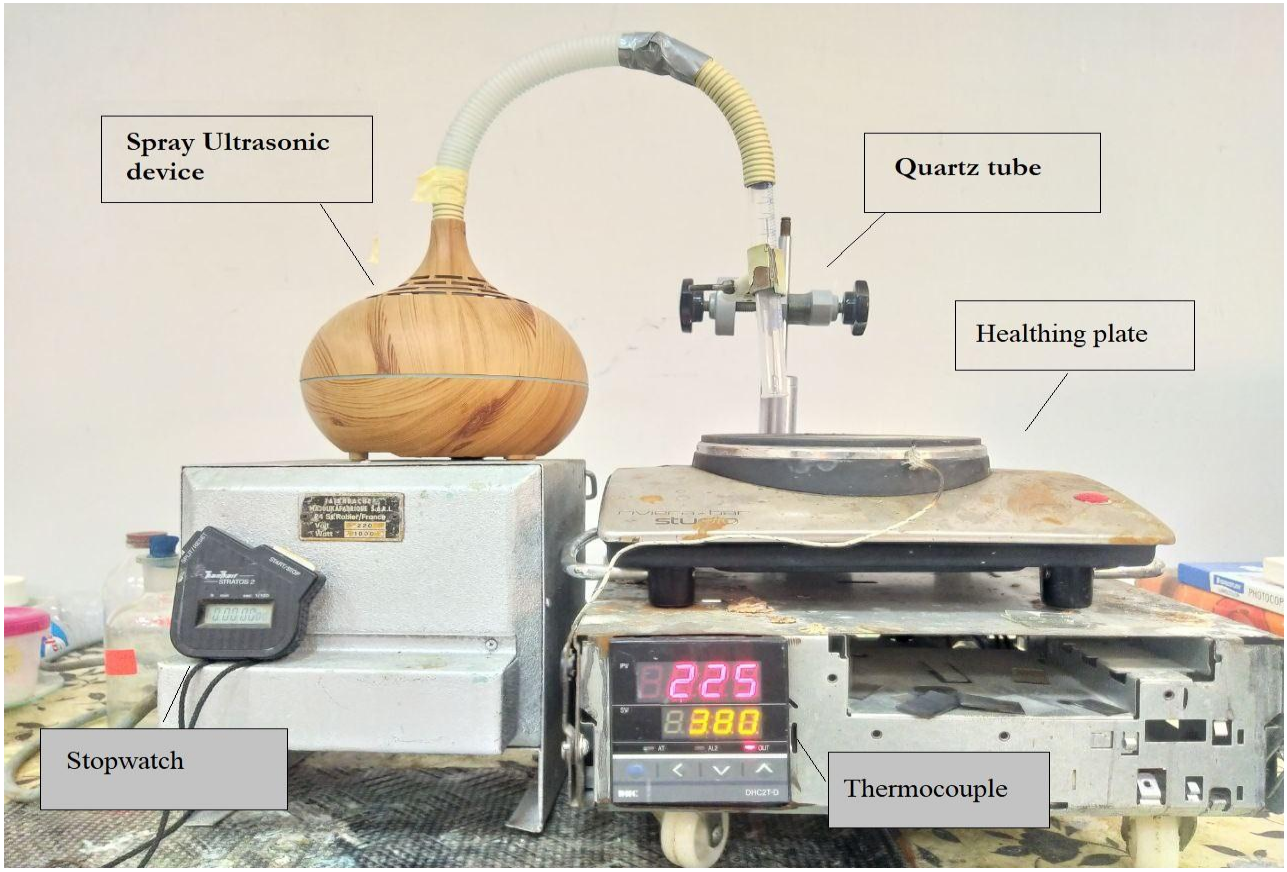

Fig. 8 The spray technique used to deposit the coating

The elements of the assembly are presented in the following:

- **ultrasonic device:** for producing the mist
- **Thermocouple:** used to control the temperature.
- **Stopwatch:** used to measure the duration of the deposition.
- **Heating system:** allows to tuning the temperature.
- **Conduction tube:** ensures the transport of fine droplets coming from the atomizer to the vicinity of the substrate.

2.Characterization techniques for thin films

2.1 X-ray diffraction

XRD measurements are conducted to determine phase composition and crystallographic properties of thin films. On the basis of XRD measurements lays the classical electromagnetic theory when an electron is oscillating in alternating electromagnetic field with the same frequency as the field. When an X-ray beam hits the atom, electrons of that atom will oscillate in the frequency of the beam. An accelerated charge emits electromagnetic radiation. In most cases the emitted radiation interferes destructively, however in the right angle of radiation the emitted radiation coincides and leaves the crystal.

Diffraction of X-rays is described by Bragg's equation: $n\lambda=2d\cdot sin\theta$ where λ is X-ray wavelength, d is interplanar distance, θ is angle of incidence with lattice plane and n is integer. X-rays with constant wavelength are radiated towards crystal lattice, radiation reflects from lattice atoms which is captured by detector.

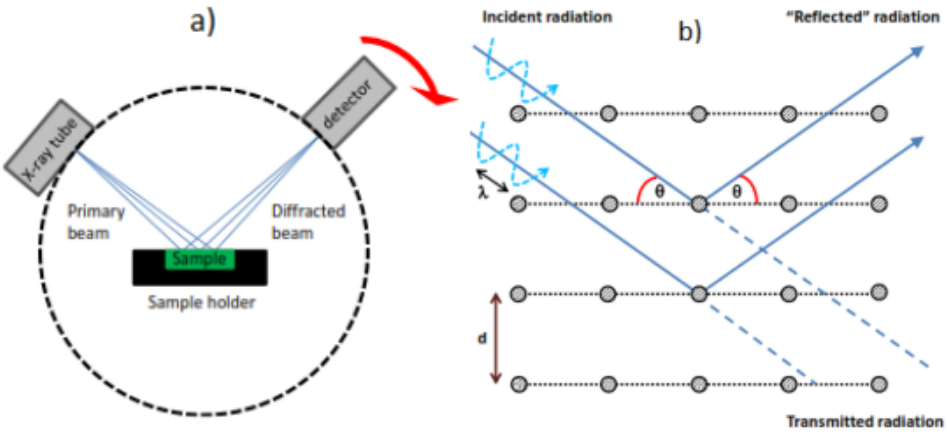

Fig. 9 a) Scheme of XRD measurement and b) Bragg's geometry of X-ray reflection

The intensity of detected radiation is plotted against 2θ. As , the angle of radiation is varied to find angles where Bragg's equationis satisfied. These angles will generate diffraction peaks in the XRD pattern and these peaks can be compared with previous experimental data giving us information of phase composition, lattice parameters and crystallites orientation. **[83]**.

2.2 Scanning electron microscope (SEM):

Scanning electron microscopy (SEM) is a topographical, compositional and elemental analysis technique where useful information about a material can be extracted based on how the material interacts with an electron beam.

An electron gun emits a beam of acceleration voltage ranging from 0.1 to 30+ keV. The beam passes through a series of electromagnetic lenses before making contact with the specimen. Different detectors measure the several types of reflected or specimen-generated beams that result from this electron-matter interaction yielding information about the specimen.

Backscattered electrons (BSE) electrons result from elastic scattering of the electron beam by the sample and give important information about spatial composition of a sample. Secondary electrons (SE) are emitted from the k-shell of the specimen atoms due to inelastic scattering of the electron beam. SE images yield high-resolution topological information about the sample. At higher acceleration voltages, the electron beam excitation can generate characteristic x-rays from atoms in the specimen. This is the basis of the Energy Dispersive X-ray Spectroscopy (EDS) technique discussed in the next section. Figure 10 presents a schematic of electron-matter interaction in SEM.

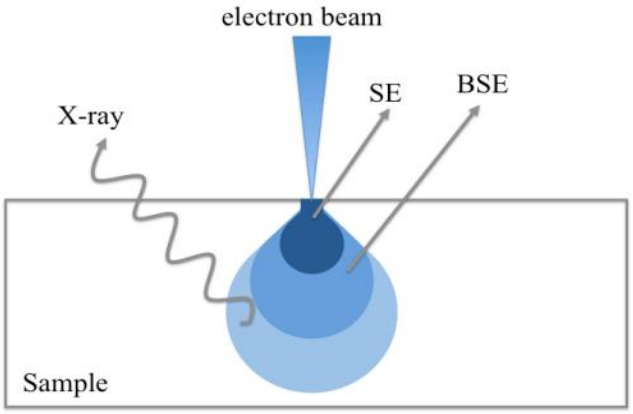

Fig. 10 Typical electron-matter interaction in SEM.

2.3 Mott–Schottky analysis

The electrochemical reactions at the electrolyte/semiconductor interface depend on the density of charge carriers at the surface of the semiconductor material, and the area of space charge. The flat band potential as well as the charge carrier density are important parameters that can be determined, in a depletion configuration interfacial, by the Mott-Schottky relation **[84]:**

$$1/(Ccs^2) = / (\varepsilon\varepsilon 0\ eN)\ (E\text{-}Etb\text{-}kT/e)$$

Where:

Ccs is the space load capacity, N the density of charge carriers, ε the dielectric constant of the semiconductor (here CuO), ε0 the electrical permittivity of vacuum, e the elementary charge, k the Boltzmann constant, T the absolute temperature, Efb the flat band potential and E the applied potential.

The plot of 1/Ccs2 as a function of E therefore makes it possible to go back, from the slope of the straight line and its abscissa at the origin, to the concentration of electrically active

dopants N and to the potential of flat bands EFB (similar to the minimum of the BC when the space charge is absent).

The Mott-Schottky analyzes were obtained for a frequency of 10 Hz. The solution electrochemical used is Na2SO4 electrolyte with a concentration of 0.25 mol/L, the speed scanning is 0.1 V/min and the potential has been varied from 0.2 to 1.2 V/ECS.

2.4. Chronopotentiometry

Chronopotentiometry (CP) is a galvanostatic method in which the current at the working electrode is held at a constant level for a given period of time. The working electrode potential and current are recorded as a function of time. Researchers employ this method to study chemical reaction mechanisms and kinetics. It is also frequently used to study batteries and electrodeposition. CP is typically performed in an unstirred electrochemical cell, although, some researchers employ rotating electrodes in conjunction with CP**[85].**

Typically, current is held constant between working and counter electrodes while potential is measured at the working electrode, relative to the reference electrode. Redox-active species diffuse to the working electrode surface to balance the applied current, until the diffusion-limited concentration of redox species reaches zero at the electrode surface, at which time potential changes to the redox potential of the next species, if present, in solution (which could be solvent). CP is also commonly used during battery charge and discharge experiments **[86].**

2.5. Electrochemical impedance spectroscopy

Electrochemical Impedance Spectroscopy (EIS) is a non-stationary method that provides information on the elementary steps that make up the overall electrochemical process. It also makes it possible to follow the evolution of the electrochemical properties of

a coated or uncoated conductive sample. EIS is a powerful technique for rapidly evaluating the performance of coated metals by measuring impedance values. It can quickly monitor changes in barrier properties of coatings compared to traditional methods. EIS also provides precise data that can be used to predict the effectiveness of a coating over time. System impedance is the ratio of the imposed sinusoidal voltage to the resulting current. It can be defined by a complex number

$$Z(\omega) = \frac{\Delta V}{\Delta I} \exp\ j\varphi$$

$$Z(\omega) = Z\exp(j\varphi) = \mathrm{Re}\,Z + j\,\mathrm{Im}\,Z$$

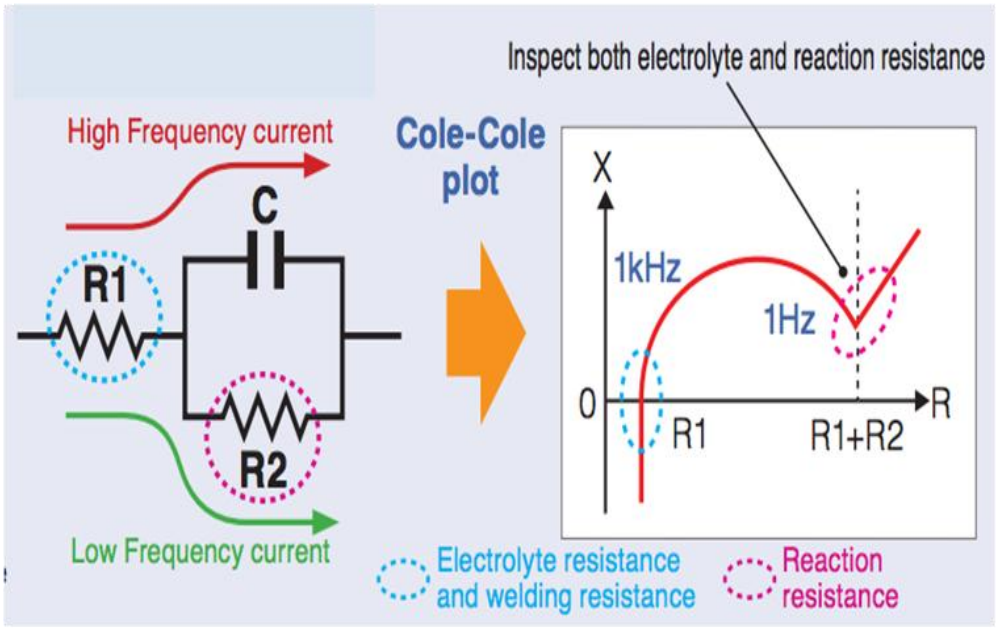

Fig. 11 Schematic representation of electrochemical impedance spectroscopy

Chapter 3

Chapter 3« Results and discussion »

1. Structural analysis

1.1. X-ray diffraction (XRD)

The structure and phase purity of undoped and Zn-doped CuO films deposited on soda lime glass substrates using ultrasonic technique were investigated using XRD (Cu-K_α radiation; wavelength: 1.5400 Å. For undoped films, the peaks at 2θ = 32.56°, 35.54°, 38.84°, 48.81°, 53.52°, 58.30°, 61.52°, 65.69°, 66.31° and 68.28° are attributed to the (110) (002) (111) (-202) (020) (202) (-113) (022) (-311) and (220) planes of CuO phase respectively according to JCPDS file no.05-0661 (figure 13). However, on can observe a diffraction peak at 2θ = 36.57°. This peak can be attributed to (111) plane corresponding to Cu_2O phase according to JCPDS file no.05-0667 (figure 14). Thus we can notice the existing of two phases (CuO and Cu_2O). No clear changes in the peak positions were evident in the diffraction data for 2 and 4% doping level. So, the substitution of Cu atoms by Zn at relatively low level atoms did not appear to have an effect on the phase formation and the structure of CuO thin films. The intensities of the (002) and (111) diffraction peaks were much stronger than those of the other peaks; thus, the film's structure appeared to have preferred crystal planes. Increasing the Zn-doping concentration resulted in a slightly change in the intensity of the diffraction peaks and also on the phase formation. Actually at 6% level, the peak located at 36.57 ° disappeared completely, which evidenced the formation of single CuO phase. At 8% level, we can see the re appearance of the peaks corresponding to Cu_2O phase.

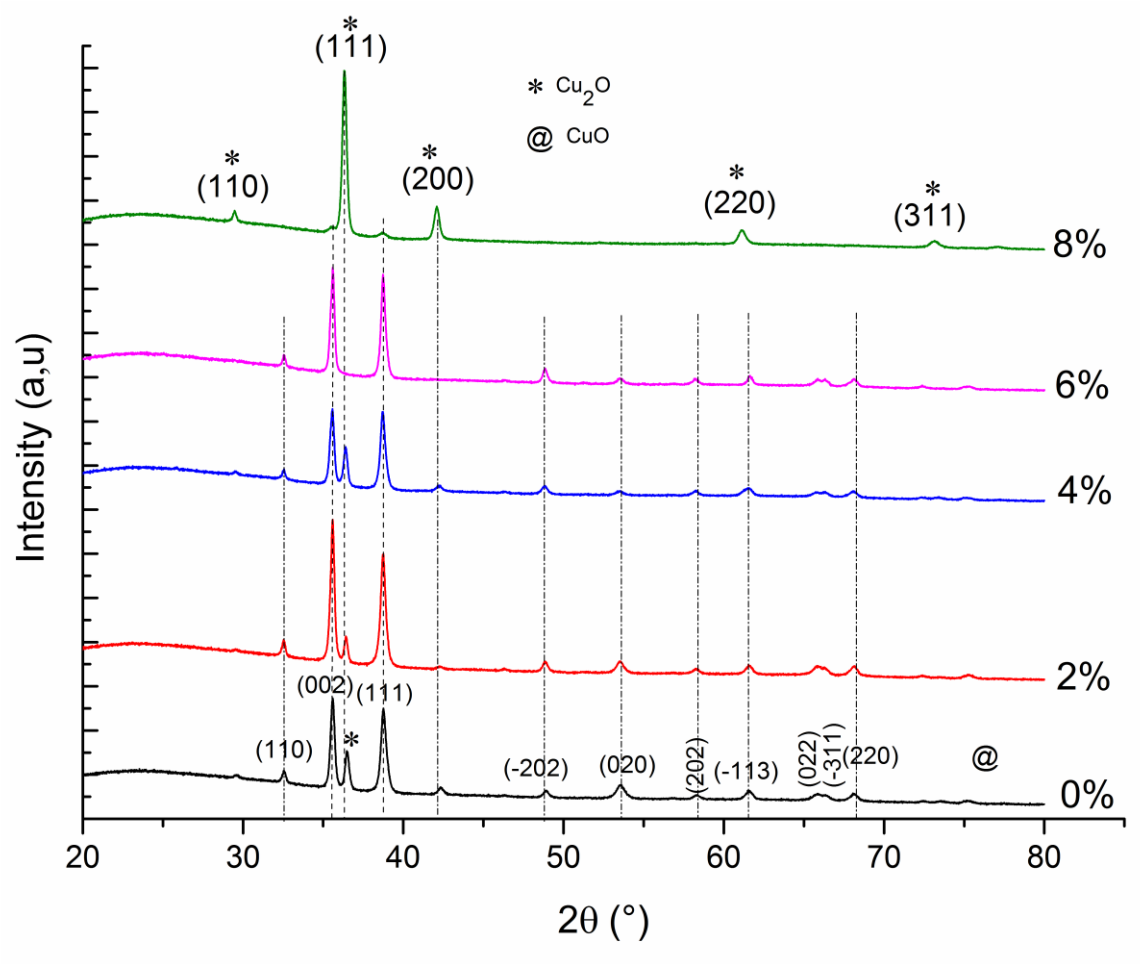

Fig. 12 XRD patterns of the undoped and Cobalt doped CuO films

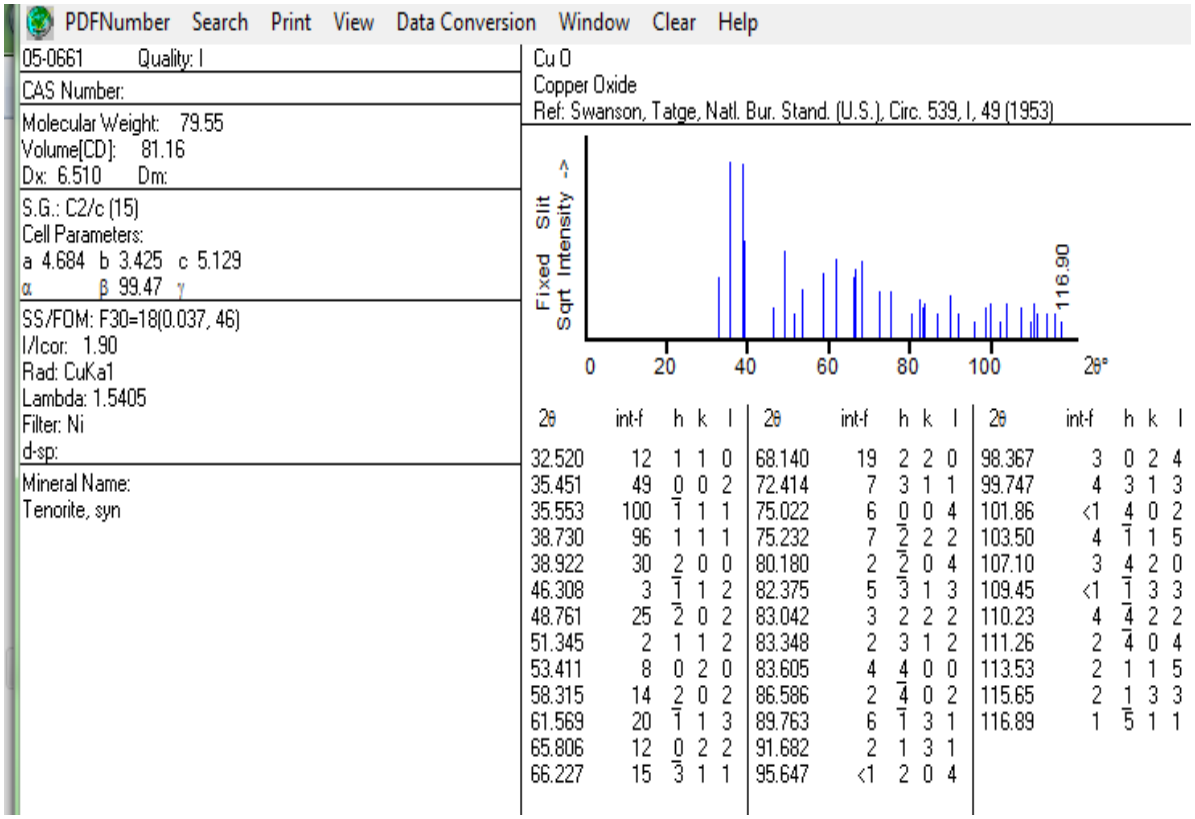

Fig. 13 PDF card no.05-0661 (CuO)

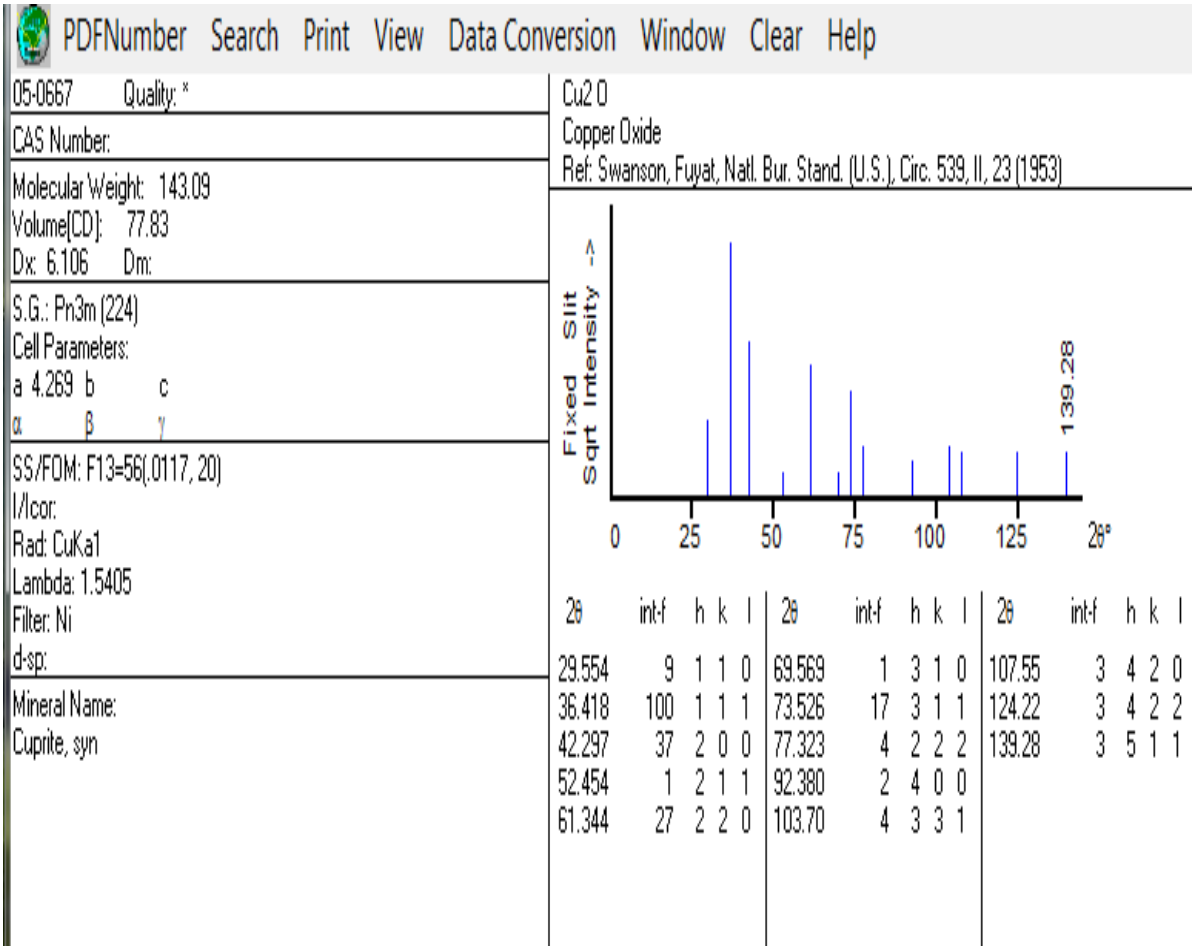

Fig. 14 PDF card no. 05-0667 (Cu_2O)

The X-ray diffraction results show clearly that the Zn inclusion plays a crucial role in the formation and crystallization of copper oxide films.

1.2. Surface morphology studies

SEM images of the thin undoped and Zn-doped CuO films are shown in Fig. 15. The surface topology of the undoped and Zn-doped CuO films was comparatively smooth, without cracks or pinholes. SEM images of 2% Zn-doped CuO films showed the formation of separate spherical grains.

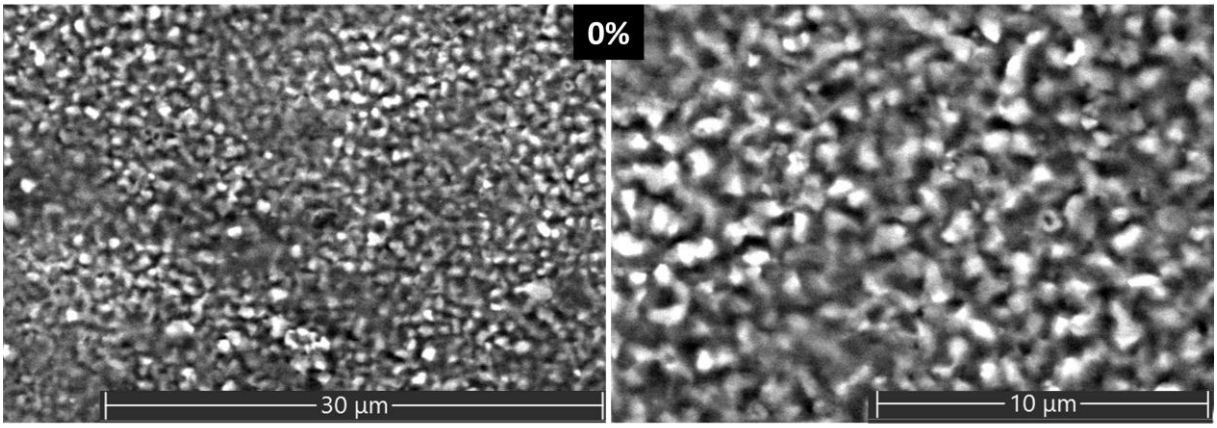
0%
30 µm
10 µm

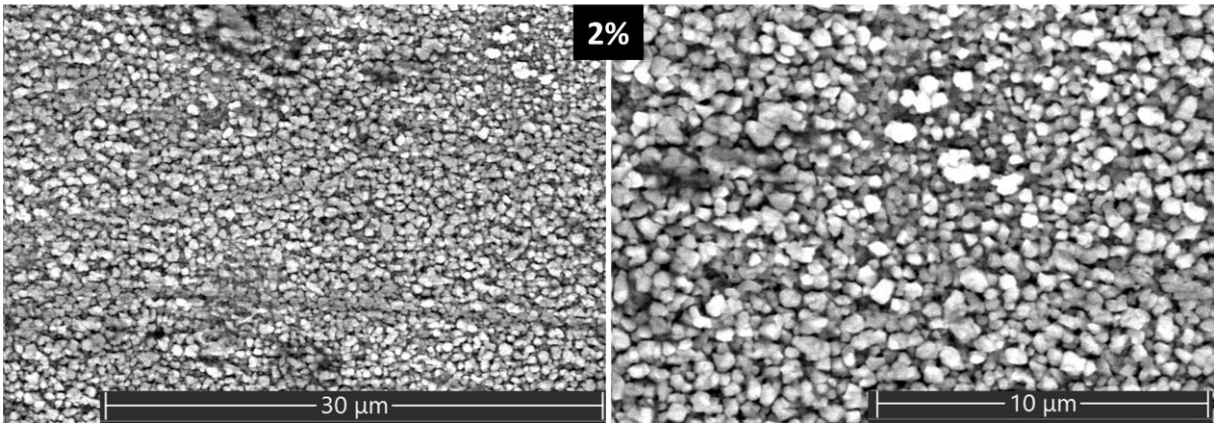
2%
30 µm
10 µm

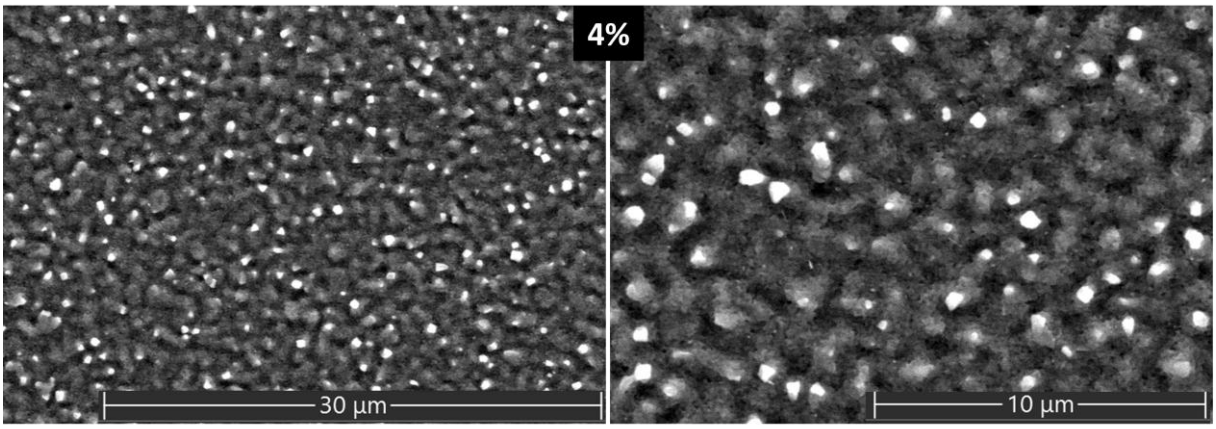
4%
30 µm
10 µm

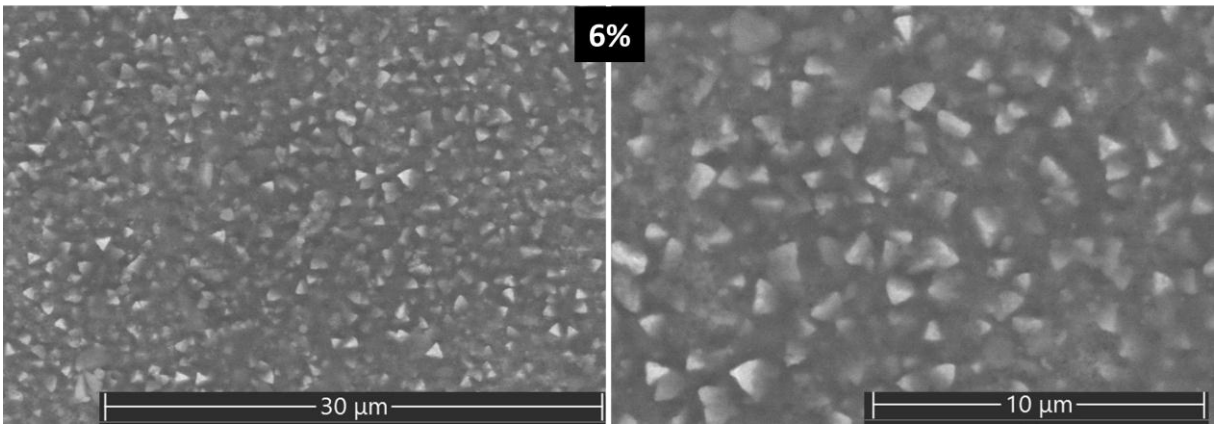
6%
30 µm
10 µm

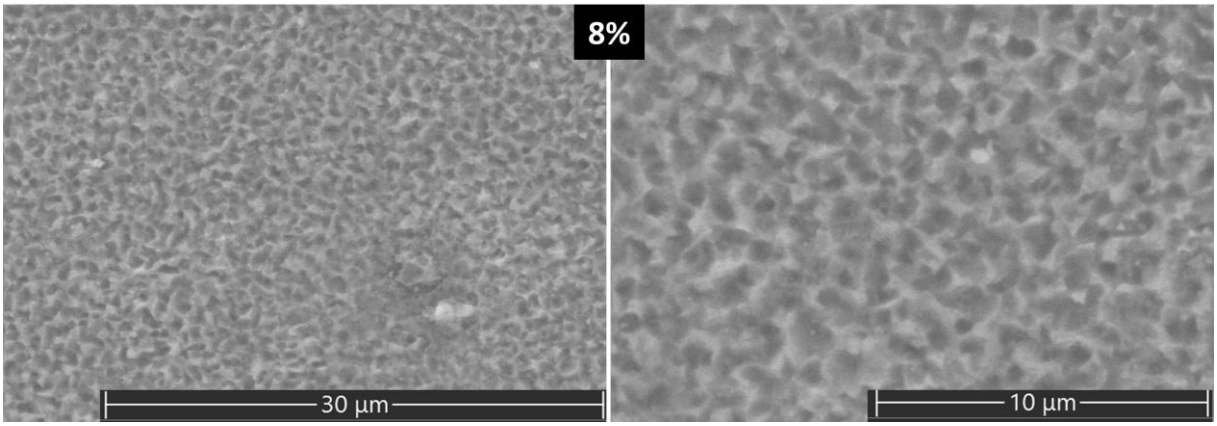

Fig. 15 SEM image of Undoped and Zn doped CuO film.

2. Electrochemical properties

2.1. Electrochemical photocurrent

Fig. 16 reports the chronoamperometry measurements (photocurrent) for pure and Zn doped CuO thin films. After switching on the light, there is a fast increase of current density, which remains then nearly constant up to when light is switched off. A good reproducibility of the results in consecutive on-off cycles can be observed. The Zn inclusion increases in general the current density excepting 6% Zn doping sample. The photocurrent of pure CuO films is about -0.02 mA. The lower photocurrent of the latter is due to the fact that the higher film thickness allows a better light harvesting, but the longer distance of photogenerated charges from the electron collector plate (on the bottom of the film) enhances the possibility of charge recombination. Thus, the photocurrent efficiency results lower. Zn doping with 4 % increases current density to -0,04 mA by increasing photo generated charges. The Zn inclusion thus strongly affects the photocurrent with respect to pure one.

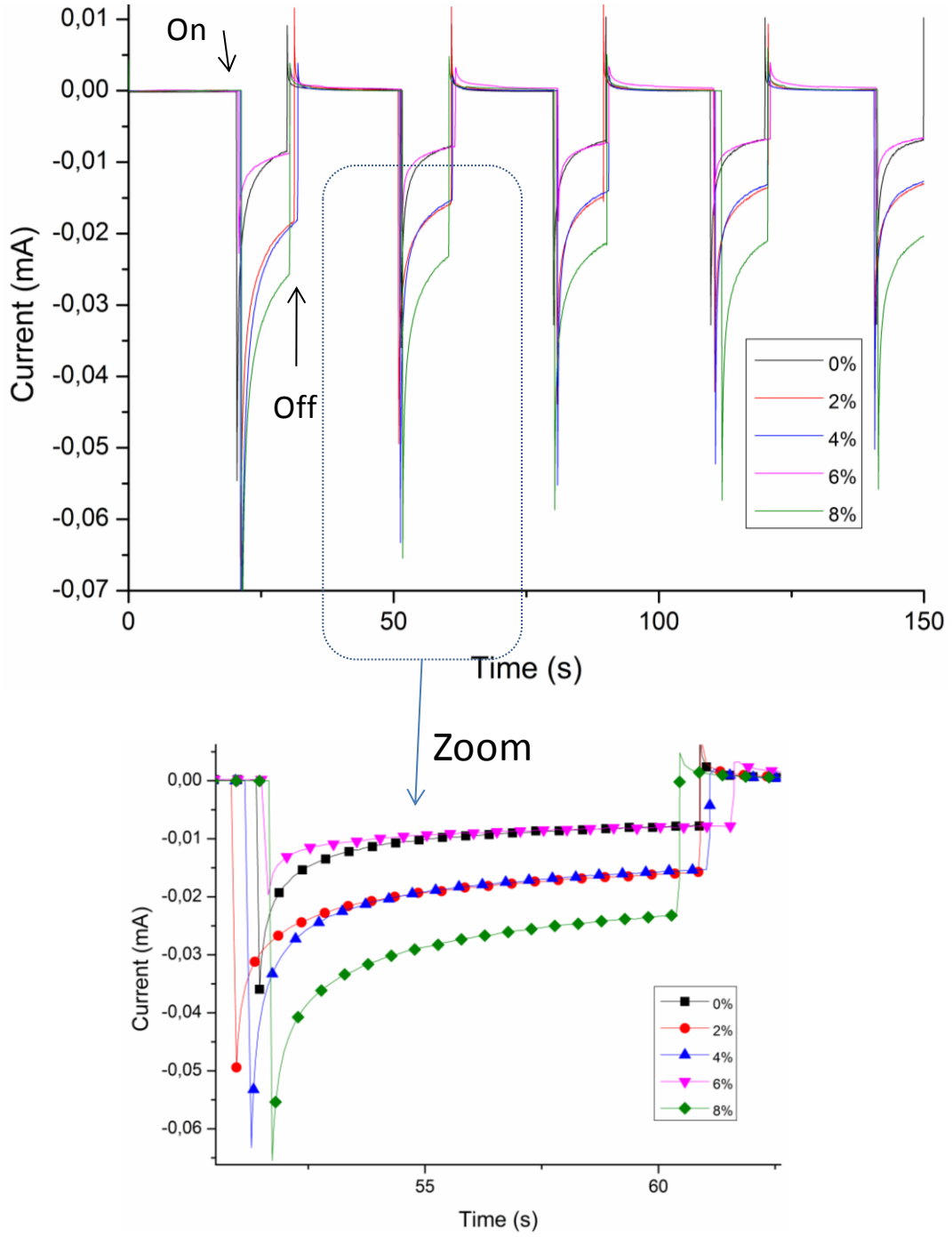

Fig. 16 Chronoamperometry measurements of Undoped and Zn doped CuO film.

2.3. Electrochemical impedance spectroscopy (EIS) study

Figure 17 shows the Nyquist diagrams of undoped and Zn doped CuO films. It can be seen from the figure that the capacitance arc radius of pure CuO films coating is larger than of all Zn doped CuO films, which means that Zn inclusion affect the charge transfer resistance of the films.

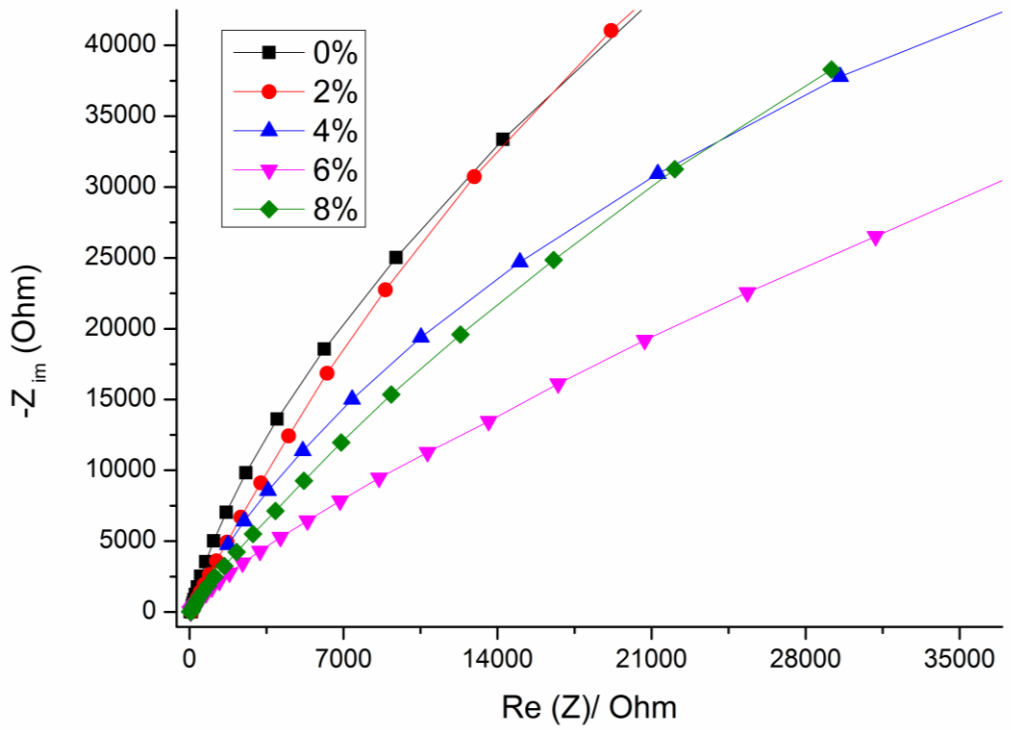

Fig. 17 Nyquist plots for the as sprayed coatings and uncoated steel disks. Exposed to 2wt% NaCl solution.

2.3. Mott-Schottky analysis

The importance of the flat band potential consists in predicting the charge transfers between the semiconductor and the electrolyte, it is necessary to know the energy levels at which these transfers take place, as well as the densities of the charge carriers available on the surface of the material (which is in contact with an electrolyte). The capacitance associated with the space charge zone is commonly evaluated by measuring the imaginary part Z" at a frequency generally fixed at 10 Hz. Thus, for a semiconductor in a depletion situation (in contact with an electrolyte), $1/C^2$ varies linearly as a function of the applied potential E. The slope of the line makes it possible to determine the density and the nature of the majority charge carriers , and its extrapolation gives the flat band potential E_{fb}.

The Mott-Schottky plots in Figure 18 show a linear part over a wide potential range, indicating the semiconductor nature of the CuO films in contact with the electrolyte. The relative line reveals a negative slope characteristic of a p-type semiconductor.

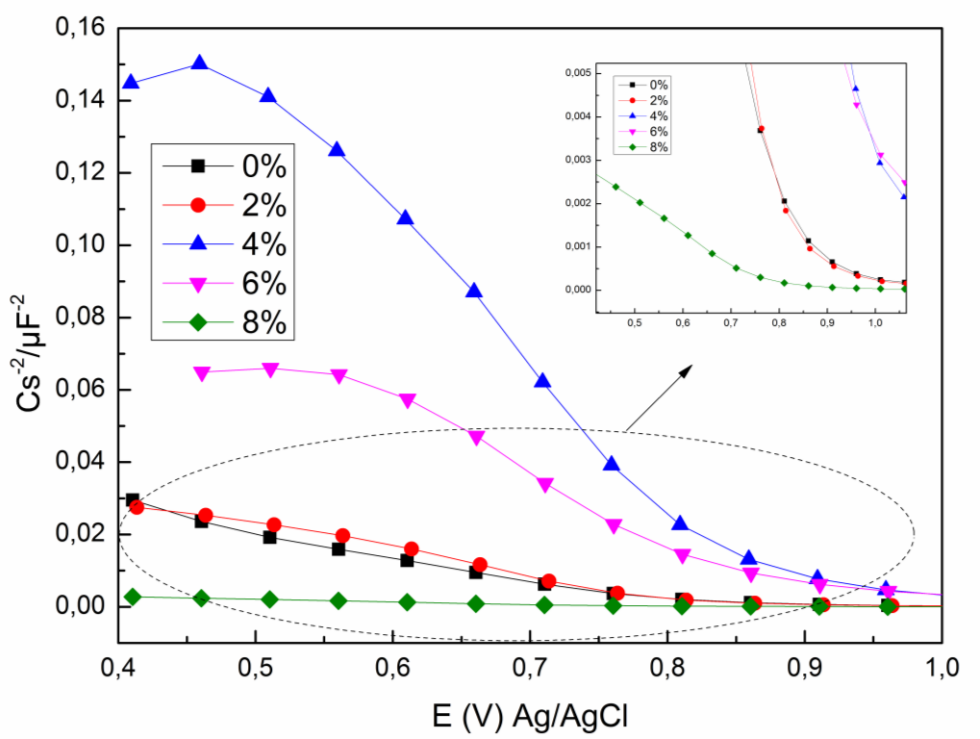

Fig. 18 Mott-Schottky curves of pure and doped CuO films

General conclusion

General conclusion

General conclusion

In this work, thin layers of pure and zinc-doped copper oxide are obtained by a chemical spray method. These layers are deposited on glass substrates and a series of samples with different levels of zinc doping is thus obtained. Several experimental techniques have been used for the characterization of these layers such as X-ray diffraction, scanning electron microscopy (SEM), and electrochemical measurements (electrochemical impedances, chronoamperometry, Mott-Schottky analysis).

Characterization by X-ray diffraction revealed that all samples are polycrystalline (pure and doped) and consist mainly of CuO and Cu2O phase. The layers crystallize in a cubic structure of (pure CuO) conforming to the reference card (JCPDS Card no.05-0661 CuO and no. 05-0667 Cu2O).

Characterization by (SEM) images of uncapped and doped zinc-coated CuO thin films. SEM images of 2% zinc-doped CuO films showed the formation of discrete spherical granules

The layers are characterized by electrochemical impedance spectroscopy and show the influence of doping on the charge transfer resistance

Copper doping leads to the appearance of a cathodic current which increases considerably for a doping rate of 8% and then decreases for a rate of 6%.

The Mott-Schottky study highlighted the variation in the potential of flat bands as a function of Zn doping. It is therefore possible to predict the density of the charge carriers for any lightly or heavily doped p-type semiconductor and in particular its n or p type.

In conclusion, we were able to develop thin layers of copper oxide by a simple chemical method and the properties of the layers obtained are considered interesting and motivating.

References

References

[01] B. Boudjema, R. Daira, A. Kabir, R. Djebien, Physico-chemical properties of CuO thin films deposited by spray pyrolysis, Inside MS 895 (2017) 33–36.

[02] A.A. Al-Ghamdi, M.H. Khedr, M. Shahnawaze Ansari, P.M.Z. Hasan, M. Sh Abdel-wahab, A.A. Farghali, RF sputtered CuO thin films: structural, optical and photo-catalytic behavior, Phys. E Low-dimens. Syst. Nanostruct. 81 (2016) 83–90.

[03] P. Samarasekara, N.T.R.N. Kumara, N.U.S. Yapa, Sputtered copper oxide (CuO) thin films for gas sensor devices, J. Phys. Condens. Matter 18 (2006) 2417–2420.

[4] H. Kidowaki, T. Oku, T. Akiyama, A. Suzuki, B. Jeyadevan, J. Cuya, Fabrication and characterization of CuO-based solar cells, JMSR 1 (2011) 138.

[05] Z. Deng, Z. Ma, Y. Li, Y. Li, L. Chen, X. Yang, H.-E. Wang, B.-L. Su, Boosting lithium-ion storage capability in CuO nanosheets via synergistic engineering of defects and pores, Front. Chem. 6 (2018) 428.

[06] Y.F. Lim, C.S. Chua, C.J. Lee, D. Chi, Sol–gel deposited Cu2O and CuO thin films for photocatalytic water splitting, Phys. Chem. Chem. Phys. 16 (2014) 25928–25934.

[07] K.U. Isah, M.I. Kimpa, J.A. Yabagi, Effect of oxidation temperature on the properties of copper oxide thin films prepared from thermally oxidised evaporated copper thin films, J. Appl. Phys. 3 (2013) 61–66.

[08] N. Serin, T. Serin, S¸. Horzum, Y. Çelik, Annealing effects on the properties of copper oxide thin films prepared by chemical deposition, Semicond. Sci. Technol. 20 (2005) 398–401.

[09]https://www.britannica.com/science/oxide

[10]G.Korotcenkov, Metal oxides for solid-state gas sensors: What determines our Choice, Materials Science and Engineering, Journal Article B: 1, (2007).

[11]P.T.Moseley BCT: Solid states gas sensors. Book. (1987).

[12]Grilli, M.L. Metal Oxides. *Metals* **2020**, *10*, 820. [**Google Scholar**] [**CrossRef**]

[13] Nunes, D.; Pimentel, A.; Santos, L.; Barquinha, P.; Pereira, L.; Fortunato, E.; Martins, R. Structural, optical, and electronic properties of metal oxide nanostructures. *Met. Oxide Nanostruct.* **2019**, 59–102. [**Google Scholar**] [**CrossRef**]

[14] Gautam, S.; Agrawal, H.; Thakur, M.; Akbari, A.; Sharda, H.; Kaur, R.; Amini, M. Metal oxides and metal organic frameworks for the photocatalytic degradation: A review. *J. Environ. Chem. Eng.* **2020**, *8*, 103726. [**Google Scholar**] [**CrossRef**]

[15]D'Anna, F.; Grilli, M.L.; Petrucci, R.; Feroci, M. WO_3 and Ionic Liquids: A Synergic Pair for Pollutant Gas Sensing and Desulfurization. *Metals* **2020**, *10*, 475. [Google Scholar] [CrossRef]

[16] Pei, C.; Han, G.; Zhao, Y.; Zhao, H.; Liu, B.; Cheng, L.; Yang, H.; Liu, S. Superior adsorption performance for triphenylmethane dyes on 3D architectures assembled by ZnO nanosheets as thin as ~1.5 nm. *J. Hazard. Mater.* **2016**, *318*, 732–741. [Google Scholar] [CrossRef]

Photochem. Photobiol. A Chem. **2016**, *315*, 25–33. [Google Scholar] [CrossRef]

[17]Yumashev, A.; Mikhaylov, A. Development of polymer film coatings with high adhesion to steel alloys and high wear resistance. *Polym. Compos.* **2020**, *41*, 2875–2880. [Google Scholar] [CrossRef]

[18]Yumashev, A.V.; Ślusarczyk, B.; Kondrashev, S.; Mikhaylov, A. Global Indicators of Sustainable Development: Evaluation of the Influence of the Human Development Index on Consumption and Quality of Energy. *Energies* **2020**, *13*, 2768. [Google Scholar] [CrossRef]

[19]Grilli, M.L.; Chevallier, L.; Di Vona, M.L.; Licoccia, S.; Di Bartolomeo, E. Planar electrochemical sensors based on YSZ with WO_3 electrode prepared by different chemical routes. *Sens. Actuators B Chem.* **2005**, *111*, 91–95. [Google Scholar] [CrossRef]

Studies. *Metals* **2020**, *10*, 598. [Google Scholar] [CrossRef]

[20] M.O'Keeffe, F.S.Stone, "The Magnetochemistry and Stoichiometry of the Copper Oxygen System", The Royal Society, (1962) 501-517.

[21] A. Aslani and V. Oroojpour, "CO gas sensing of CuO nanostructures, synthesized by an assisted solvothermal wet chemical route,"Physica B: Condensed Matter,vol.406,no.2,pp.144–149,2011.

[22]M.Yang,J.He,X.Hu,C.Yan,andZ.Cheng,"CuOnanostructures as quartz crystal microbalance sensing layers for detection

of trace hydrogen cyanide gas,"Environmental Science and

Technology,vol.45,no.14,pp.6088–6094,2011.

[23] H. Zhang and M. Zhang, "Synthesis of CuO nanocrystalline and their application as electrode materials for capacitors,"Materials Chemistry and Physics,vol.108,no.2-3,pp.184–187,2008.

[24]Z.Wang,F.Su,S.Madhavi,andX.W.Lou,"CuOnanostructures

supported on Cu substrate as integrated electrodes for highly

reversible lithium storage,"Nanoscale,vol.3,no.4,pp.1618–

1623, 2011.

[25] A. K. Rai, L. T. Anh, J. Gim et al., "Facile approach to synthesize CuO/reduced graphene oxide nanocomposite as anode materials for lithium-ion battery,"Journal of Power Sources,vol.244, pp.435–441,2013.

[26] Y. Yecheskel, I. Dror, and B. Berkowitz, "Catalytic degradation of brominated flame retardants by copper oxide nanoparticles," Chemosphere,vol.93,no.1,pp.172–177,2013.

[27] H. Kidowaki, T. Oku, T. Akiyama, A. Suzuki, B. Jeyadevan, and J. Cuya, "Fabrication and characterization of CuO-based solar cells,"Journal of Materials Science Research,vol.1,no.1,pp.138– 143, 2012.

[28] S. Chandrasekaran, "A novel single step synthesis, high efficiency and cost effective photovoltaic applications of oxidized copper nano particles,"Solar Energy Materials and Solar Cells, vol. 109, pp. 220–226, 2013.

[29] K. Han and M. Tao, "Electrochemically deposited p-n homojunction cuprous oxide solar cells," Solar Energy Materials and Solar Cells,vol.93,no.1,pp.153–157,2009.

[30] S. Anandan, X. Wen, and S. Yang, "Room temperature growth of CuO nanorod arrays on copper and their application as a cathode in dye-sensitized solar cells,"Materials Chemistry and Physics,vol.93,no.1,pp.35–40,2005.

[31] Y. Liu, L. Liao, J. Li, and C. Pan, "From copper nanocrystalline to CuO nanoneedle array: synthesis, growth mechanism, and properties,"Journal of Physical Chemistry C, vol. 111, no. 13, pp. 5050–5056, 2007.

[32] Y. Liu, L. Zhong, Z. Peng, Y. Song, and W. Chen, "Field emission properties of one-dimensional single CuO nanoneedle by in situ microscopy,"Journal of Materials Science,vol.45,no.14,pp. 3791–3796, 2010.

[33] R.-C. Wang and C.-H. Li, "Improved morphologies and
enhanced field emissions of CuO nanoneedle arrays by heating
zno coated copper foils,"Crystal Growth and Design,vol.9,no.
5, pp. 2229–2234, 2009.

[34] L. Hu, D. Zhang, H. Hu, and T. Guo, "Field electron emission
from structure-controlled one-dimensional CuO arrays synthesized by wet chemical process,"Journal of Semiconductors,vol. 35,no.7,ArticleID073003,pp.1–4,2014.

[35] Y.W.Zhu,C.H.Sow,andJ.T.L.Thong,"Enhancedfieldemission from CuO nanowire arrays by in situ laser irradiation,"
Journal of Applied Physics,vol.102,ArticleID114302,2007.

[36]S.K.Maji,N.Mukherjee,A.Mondal,B.Adhikary,andB.Karmakar, "Chemical synthesis of mesoporous CuO from a single
precursor: structural, optical and electrical properties,"Journal
of Solid State Chemistry,vol.183,no.8,pp.1900–1904,2010.

[37] Kittel, "Introduction `a la physique de l'´etat solide", (1974).

[38]] C. Li, G. Song, Photocatalytic degradation of organic pollutants and detection of chemical oxygen demand fluorescence method, Sens. Actuators B 137 (2) (2009) 432–436.

[39] G. Chaitanya Lakshmi, S. Ananda, R. Somashekar, C. Ranganathiah, Synthesis, characterization and photocatalytic activity of ZnO: sn nanocomposites, Int. J. Adv. Sci. Technol. 5 (2012) 54–64

[40] Q.zhu, Y. Zhang, J. Wang, Microwave synthesis of cuprous oxide micro/nanocrystals with different morphologies and photocatalytic activities, J. Mater. Sci. Technol. 27 (2011) 289–295.

[41] F.P. García de Arquer, D.V. Talapin, V.I. Klimov, Y. Arakawa, M. Bayer, E.H. Sargent, Semiconductor quantum dots: Technological progress and future challenges, Science 373 (2021) eaaz8541. https://www.science.org/doi/10.1126/ science.aaz8541.

[42] R.S. Ohl, Light-sensitive electric device, U.S. Patent US2402662A, 1941 May 27.

[42]] S.J. Fonash, Chapter Five - Semiconductor–semiconductor Heterojunction Cells, in: S.J. Fonash (Ed.), Solar Cell Device Physics, second ed., Academic Press, Boston, 2010, pp. 183–262.

[43] H.B. Michaelson, The work function of the elements and its periodicity, J. Appl. Phys. 48 (1977) 4729–4733, https://doi.org/10.1063/1.323539.

[44] A. Sahu, B. Russ, M. Liu, F. Yang, E.W. Zaia, M.P. Gordon, J.D. Forster, Y.-Q. Zhang, M.C. Scott, K.A. Persson, N.E. Coates, R.A. Segalman, J.J. Urban, In-situ resonant band engineering of solution-processed semiconductors generates high performance n-type thermoelectric nano-inks, Nat. Commun. 11 (2020) 2069, https://doi.org/10.1038/s41467-020-15933-2.

[45] E. Lhuillier, P. Guyot-Sionnest, Recent Progresses in Mid Infrared Nanocrystal Optoelectronics, IEEE J. Sel. Topics Quantum Electron. 23 (2017) 6000208. https://ieeexplore.ieee.org/document/7891991.

[46] P.R. Brown, D. Kim, R.R. Lunt, N.i. Zhao, M.G. Bawendi, J.C. Grossman, V. Bulovi´c, Energy Level Modification in Lead Sulfide Quantum Dot Thin Films through Ligand Exchange, ACS Nano 8 (2014) 5863–5872, https://doi.org/10.1021/nn500897c.

[47] A. Zunger, O.I. Malyi, Understanding Doping of Quantum Materials, Chem. Rev. 121 (2021) 3031–3060, https://doi.org/10.1021/acs.chemrev.0c00608.

[48] D.J. Norris, A.L. Efros, S.C. Erwin, Doped Nanocrystals, Science 319 (2008) 1776, https://doi.org/10.1126/science.1143802.

[49] G. Zhang, B. Kirk, L.A. Jauregui, H. Yang, X. Xu, Y.P. Chen, Y. Wu, Rational Synthesis of Ultrathin n-Type Bi2Te3 Nanowires with Enhanced Thermoelectric Properties, Nano Lett. 12 (2012) 56–60, https://doi.org/10.1021/nl202935k.

[50] T. Michely and J. Krug. Islands, Mounds and Atoms: Patterns and Processes in Crystal Growth far from Equilibrium. Springer-Verlag, Berlin Heidelberg (2003).

[51] Z. Zhang and M. G. Lagally. Science (80-.). 276 (1997) 377.

[52] C. V. Thompson. Annu. Rev. Mater. Sci. 30 (2000) 159

[53] G. Koster, G. J. H. M. Rijnders, D. H. A. Blank, and H. Rogalla. Appl. Phys. Lett. 74 (1999) 3729.

[54] I. Petrov, P. B. Barna, L. Hultman, and J. E. Greene. J. Vac. Sci. Technol. A 21 (2003) S117.

[55] B. A. Movchan and A. V. Demchishin. Phys. Met. Metallogr. 28 (1969) 653.

[56] A. Anders. Thin Solid Films 518 (2010) 4087.

[57] Fu-Chien Chiu, Tung-Ming Pan, Tapas Kumar Kundu and Chun-Hsing Shih, Thin Film Applications in Advanced Electron Devices, Advances in Materials Science and Engineering, vol. 2014, p. 927358 (2014)

[58] M. C. Rao and M. S. Shekhawat, A BRIEF SURVEY ON BASIC PROPERTIES OF THIN FILMS FOR DEVICE APPLICATION, International Journal of Modern Physics: Conference Series, vol. 22, 576-582 (2013)

[59] Hartmut Frey and Hamid R. Khan: Handbook of Thin Film Technology. (Berlin, Heidelberg: Springer Berlin/ Heidelberg, Berlin, Heidelberg, 2015).

[60] John R. Arthur, In Specimen Handling, Preparation, and Treatments in Surface Characterization, ed. Alvin W. Czanderna, Powell Cedric J., Madey Theodore E., Hercules David M. and Yates John T. (Springer US: Boston, MA, 1998), pp. 239-293.

[61] K. L. Choy, Chemical vapour deposition of coatings, Progress in Materials Science, vol. 48, 57-170 (2003)

[62] Milton Ohring: The materials science of thin films / Milton Ohring. (Academic Press Harcourt Brace Jovanovich Publ, San Diego New York Boston (Mass.) [etc, 1992).

[63] S. Kozhukharov, S. Tchaoushev, Journal of Chemical Technology and Metallurgy, 48 (2013) 111-118.

[64] L. Filipovic, S. Selberherr, G. C. Mutinati, E. Brunet, S. Steinhauer, A. Kock, J. Teva, J. Kraft, J. Siegert, and F. Schrank, Proceedings of the World Congress on Engineering (WCE), II (2013) 987-992.

[65] C. Zengjun. TIO2 Thin films by ultrasonic spray pyrolysis. Tallinn university of technology School of Engineering Department of Materials and Environmental Technology.

[66] R.R. Chamberlein, J.S. Skarman. Chemical spray deposition process for inorganic films, J. Electrochem. Soc., 113 (1) (1966) 86–89.

[67]. L Filipovic, M Ianeng, S Selberherr, GC Mutinati, E Brunet, S Steinhauer, A Köck, J Teva, J Kraft, J Siegert, F Schrank. Modeling Spray Pyrolysis Deposition, Proceedings of the World Congress on Engineering, 2013, Vol.2.

[68] S.P.S. Arya, H.E. Hintermann. Growth of Y-Ba-Cu-O superconducting thin films by ultrasonic spray pyrolysis, Thin Solid Films, 193 (1990) 841–846.

[69] H. Yoon, J.H. Woo, Y.M. Ra, S.S. Yoon, H.Y. Kim, S.J. Ahn, J.H. Yun, J. Gwak, K.H. Yoon, S.C. James. Electrostatic spray deposition of copper-indium thin films, Aerosol Sci. Techn., 45 (2011) 1448–1455.

[70] P. Svetlana. Tin Sulfide Films by Chemical Spray Pyrolysis: Formation and Properties. Tallinn University of Technology School of Engineering Department of Materials and Environmental Technology.

[71] S Pramod. Patil. Versatility of chemical spray pyrolysis technique. Materials Chemistry and Physics, 1999,vol. 59, p. 185-198.

[72] A. J. C. Fiddes, Deposition of zinc oxide by spray pyrolysis, doctoral thesis, Durham University, 1993.

[73] M. Dobre and L. Bolle, Theoretical prediction of ultrasonic spray characteristics using the maximum entropy formalism, ILASS-Europe'98 Manchester, 1998.

[74]G.Korotcenkov,V. Brinzari,J. Schwank,M. DiBattista,andA. Vasiliev, Sensors and Actuators B: Chemical, 77 (2001) 244-252.

[75] D. Perednis and L. J. Gauckler, Solid State Ionics, 166 (2004) 229-239.

[76] S. H. Ng, J. Wang, D. Wexler, S. Y. Chew, and H. K. Liu. . The Journal of Physical Chemistry C, 111 (2007) 11131-11138.

[77] G. Blandenet,M.Court,andY. Lagarde, Thin Solid Films, 77 (1981) 81-90.

[78] Y. Benkhetta et al Optik 127 (2016) 3005–3008.

[79] J.E. Hill and R.R. Chamberlin, US Patent 3, 148 (1964) 084

[80] M. S. Sameem, IJRSET, II (2015) 19-24.

[81] A.Taabouche, A. Bouabellou, F. Kermiche, F. Hanini, S. Menakh, Y. Bouachiba, T. Kerdja,C. Benazzouz, M. Bouafia, S. Amara, Materials Physics and Chemistry, 3 (2013) 209-213.

[82] M. S. Sameem, IJRSET, II (2015) 19-24

[83] T. Srinivasulu, K. Saritha, K.T. R. Reddy, Modern Electronic Materials, 3 (2017) 76- 85.

[84] D. Perednis& J. Ludwig, G auckler. Thin Film Deposition Using Spray Pyrolysis Nonmetallic Inorganic Materials, Department of Materials, Swiss Federal Institute of Technology, Wolfgang-PauliStr. 10, CH-8093 Zurich, Switzerland.

[85] K. Darowicki, S. Krakowiak, P. Slepski, Electrochimica Acta 51 (2006) 2204–2208

[86] Kissinger, P.; Heineman, W. R. Laboratory Techniques in Electroanalytical Chemistry, 2nd ed. Marcel Dekker, Inc: New York, 1996.

Abstract

Abstract

ملخص

في هذه المذكرة قمنا بدراسة تفصيلية لعينات من أكسيد النحاس، تم تحضيرها باستخدام تقنية الرش الكيميائي. وقد استعنا في هذا البحث بعدة تقنيات تسمح بدراسة الخواص البنيوية المجهرية والضوئية للعينات المحضرة. وتشمل هذه التقنيات مايلي: الحيود السيني وقياسات الخصائص الضوئية. بينت أطياف الحيود السيني أن حبيبات أكسيد النحاس التي تتكون منها الشرائح تتمتع بخصائص بلورية غير موجهة . هذه الرقائق لها امتصاصية كبيرة في المجال المرئي. تبين من خلال هذه الدراسة أن الاشابة بعنصر النحاس ستؤثر على التيار الضوئي الناتج و طبيعة المادة الناتجة.

الكلمات المفتاح: أكسيد النحاس، الحيود السيني ، الرش الكيميائي ، خصائص ضوئية، التيار الضوئي

Abstract

In this note, we study in detail samples of copper oxide, which were prepared using chemical spraying technique. We have used

In this research, there are several techniques that allow studying the microstructural and optical properties of the prepared samples. These technologies include

Miley: sigmoidal diffraction and optical properties measurements. The sigmoidal diffraction spectra indicated that the copper oxide grains that make up it

The chips have non-oriented crystal properties. These chips have a large absorbance in the visible field. Show through this

The study is that doping with copper will affect the resulting photocurrent and the nature of the resulting material.

Key words: copper oxide, x-diffraction, chemical spraying, optical properties, photocurrent